

REVIEW

Open Access



Nanomedicine's shining armor: understanding and leveraging the metal-phenolic networks

Zhengming Tang¹ , Zhijie Huang¹, Yisheng Huang², Mingshu Huang¹, Hongyu Liu¹, JianZhong Du^{3,4*†} and Bo Jia^{1*†}

Abstract

Metal-phenolic networks (MPNs), which comprise supramolecular amorphous networks formed by interlinking polyphenols with metal ions, garner escalating interest within the realm of nanomedicine. Presently, a comprehensive synthesis of the cumulative research advancements and utilizations of MPNs in nanomedicine remains absent. Thus, this review endeavors to firstly delineate the characteristic polyphenols, metal ions, and their intricate interaction modalities within MPNs. Subsequently, it elucidates the merits and demerits of diverse synthesis methodologies employed for MPNs, alongside exploring their potential functional attributes. Furthermore, it consolidates the diverse applications of MPNs across various nanomedical domains encompassing tumor therapy, antimicrobial interventions, medical imaging, among others. Moreover, a meticulous exposition of the journey of MPNs from their ingress into the human body to eventual excretion is provided. Lastly, the persistent challenges and promising avenues pertaining to MPNs are delineated. Hence, this review offering a comprehensive exposition on the current advancements of MPNs in nanomedicine, consequently offering indirect insights into their potential clinical implementation.

Keywords Nanomedicine, Metal-polyphenol networks, Polyphenols, Polyphenol-containing structures

[†]JianZhong Du and Bo Jia have contributed equally to this work.

*Correspondence:

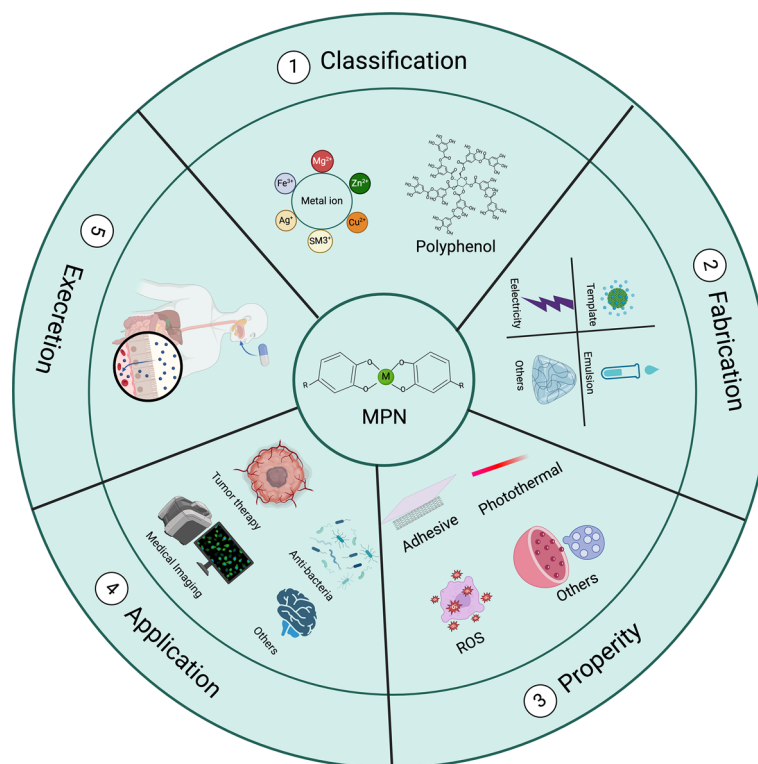
JianZhong Du
jzdu@tongji.edu.cn
Bo Jia
dentist-jia@163.com

Full list of author information is available at the end of the article



© The Author(s) 2025. **Open Access** This article is licensed under a Creative Commons Attribution-NonCommercial-NoDerivatives 4.0 International License, which permits any non-commercial use, sharing, distribution and reproduction in any medium or format, as long as you give appropriate credit to the original author(s) and the source, provide a link to the Creative Commons licence, and indicate if you modified the licensed material. You do not have permission under this licence to share adapted material derived from this article or parts of it. The images or other third party material in this article are included in the article's Creative Commons licence, unless indicated otherwise in a credit line to the material. If material is not included in the article's Creative Commons licence and your intended use is not permitted by statutory regulation or exceeds the permitted use, you will need to obtain permission directly from the copyright holder. To view a copy of this licence, visit <http://creativecommons.org/licenses/by-nc-nd/4.0/>.

Graphical Abstract



Introduction

Nanomedicine comprises a multidisciplinary area of study that has emerged in recent decades, primarily involving the use of engineered nanocarriers to transport nanodrugs for preventing, diagnosing, and treating diseases to achieve medical benefits [1–3]. Presently, nanomedicine utilizes nanomaterials that encompass both organic substances (e.g., liposomes) and inorganic substances (e.g., metal nanoparticles). These nanomaterials have sizes ranging from 1 to 1000 nm and exhibit diverse shapes such as spherical, tubular, and rod-shaped, among others [4–6]. When compared to traditional drugs, nanodrugs and their carriers offer several distinct advantages. These include the ability to effectively penetrate biological barriers, transport hydrophobic drugs, bind with bioactive molecules like DNA and proteins, target specific disease sites, improve the absorption of oral medications, and possess unique physicochemical properties such as particle size and surface modification [7, 8]. By leveraging these advantages, nanomedicine offers a diverse array of uses, such as drug delivery, disease diagnosis and imaging, biomarkers, and regenerative

medicine, among others [3, 9]. Despite its vast potential, nanomedicine still faces several limitations and challenges, including effective drug delivery to diseased areas (e.g., solid tumors), characterization analysis of composite nanomaterials, large-scale production of nanomaterials, and the pharmacology and biosafety of nanomaterials [10, 11]. Hence, it is imperative to prioritize the development of nanomaterials that are safer, more effective, capable of accurately targeting desired sites, and readily producible to propel the progress of nanomedicine and enhance human well-being.

Polyphenols comprise a class of organic compounds with multiple phenolic hydroxyl groups that are commonly found in different types of food and have various functions, including anti-inflammatory, antioxidant, and antibacterial properties, among others [12, 13]. Moreover, the existence of pyrogallol groups in polyphenol molecules enables them to create complexes with different kinds of metals, including transition metals and metal salts, when in a liquid state [14]. Due to these properties, there has been a growing research interest in the polyphenol-containing structures [15–17].

Metal-Polyphenol Networks (MPNs), which comprise supramolecular amorphous networks formed by interlinking polyphenols with metal ions, have gained significant attention in the field of polyphenol studies due to their exceptional physicochemical properties [18]. In this context, studies conducted by Caruso et al., at the University of Melbourne demonstrated that natural polyphenols and metal ions have the ability to rapidly chelate on various solid surfaces and self-assemble into supramolecular three-dimensional network structures [19, 20]. Contrary to metal-free polyphenolic nano assemblies, MPNs highly benefit from the synergistic interaction between the metal ions and polyphenols that constitute their structure; As a result, they demonstrate superior functional properties [21]. The attributes of metal ions also enable the advancement of numerous optimal materials, in which different metal ions frequently introduce entirely distinct functionalities.

Due to these structural characteristics, MPNs possess several advantages over other nanomaterials. In contrast to Metal Organic Frameworks (MOFs), MPNs are synthesized using simpler and more environmentally friendly methods, while MOFs typically require more stringent conditions and result in higher expenses [19, 21]. Furthermore, MPNs exhibit greater efficacy in applications such as tissue regeneration, photothermal conversion, and conferring specific magnetic properties, in comparison to MOFs [22, 23]; Moreover, the phenolic hydroxyl in the organic ligands of MPNs enable effective adsorption onto substances with any topographic characteristics [18, 24, 25]; Additionally, metal ions in MPNs provide supplementary functionalities such as medical imaging, photothermal conversion, and antimicrobial properties, which is in contrast to pure polyphenolic substances [26–29]; Furthermore, when compared to other nano-composite materials, the MPNs demonstrate dissociation of metal ions from polyphenols at low pH levels, while maintaining stability under normal physiological conditions. This stability allows MPNs to circulate within the body for extended periods of time and enables targeted drug delivery. MPNs are a category of materials that have great potential in the field of nanomedicine.

So far, reviews about MPNs have predominantly focused on their use in specific areas of nanomedicine, like tumor therapy and antimicrobial applications [30, 31], or examined the development and applications of MPNs in nanomedicine using specific types of polyphenols or metal ions [32, 33]. Correspondingly, there has been a lack of comprehensive reviews that summarize the overall progress and practical uses of MPNs in the field of nanomedicine. Hence, this review aims to provide a comprehensive overview of the structural

characteristics, synthesis techniques, and functional attributes of MPNs, as well as their diverse applications and biological outcomes in the field of nanomedicine. Firstly, we introduce the typical types and functional attributes of the various constituents (polyphenols, metal ions) found in MPNs, as well as the nature of their combinations. Subsequently, we outline the conventional techniques used for assembling MPNs. In addition, we provide concise overview of the functional properties of different MPNs, such as their adhesiveness, responsiveness to changes in pH, ability to escape from lysosomes, photothermal conversion propriety and so on. This is followed by a compilation of the diverse applications of MPNs in various nanomedical disciplines. Thereafter, we review the typical biological pathways of MPNs within the body. Finally, we examine the existing constraints on research regarding MPNs and propose potential avenues for future investigations. Overall, this review offers a comprehensive overview of the design, preparation, application, biological fate, and potential of MPNs in the field of nanomedicine, with the aim to provide novel insights for future research and promote successful clinical implementation.

Metal-phenolic networks

Polyphenols

The classical definition of polyphenols is that “Only substances bearing a large enough number of di- and/or trihydroxyphenyl units, by virtue of either their oligomeric nature or the multiple display of these phenolic motifs in their monomeric forms, can fit the definition as long as they remain soluble in water” [12]. There exists a multitude of common methodologies for the classification of polyphenols, including categorization by molecular weight, source of the substance, and chemical structure, among others. Firstly, classification by molecular weight can be subdivided into: high-molecular-weight polyphenols, which refer to those with a molecular weight between 500 and 4000 Da and containing 5–7 phenolic rings per 1000 Da [12], and low-molecular-weight polyphenols generally referring to those with at least two hydroxyl groups or more than one phenolic ring in their structure [31]; Secondly, classification by chemical structure differentiates polyphenols into flavonoids, phenolic acids, stilbenes, lignans, and other classes [34]; Thirdly, classification by source divides polyphenols into natural polyphenols and synthetic polyphenols. To facilitate a better understanding of the function and application prospects of polyphenols in MPN nanomedicine, we will elaborate on the current common types of polyphenols based on their source, along with their functional characteristics.

Natural polyphenols

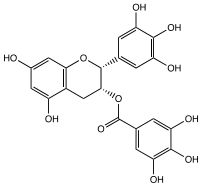
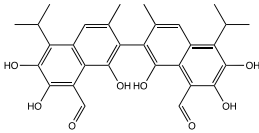
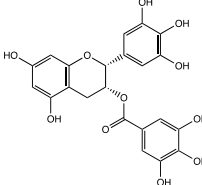
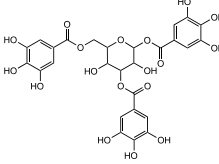
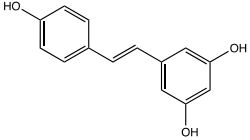
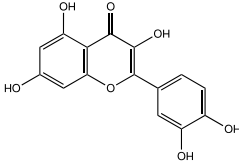
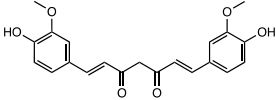
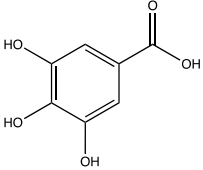
Natural polyphenols are secondary metabolites derived from plants, typically containing one or more phenolic rings in their structure, providing protective roles against oxidative damage [35]. Besides, the biological activities of natural polyphenols include anti-inflammatory, anti-cancer, cardioprotective, neuroprotective, and anti-aging effects [36]. Common natural polyphenols include tannic acid (TA), quercetin, resveratrol, curcumin, tea polyphenols, and gossypol, among others (Table 1).

Tea polyphenols are the principal active components found in tea, primarily comprising catechins, anthocyanins (ACN), and other polyphenolic compounds. Catechins account for 60–80% of tea polyphenols and are categorized into four types: epicatechin (EC), epicatechin gallate (ECG), epigallocatechin (EGC), and epigallocatechin gallate (EGCG) [37]. Predicated upon their chemical structure, catechins are predominantly recognized for their antioxidant activities [38]. There has been considerable research demonstrating that catechins play a crucial role in anti-inflammatory processes, prevention of cardiovascular diseases, and cancer therapy [39, 40]. Another class of tea polyphenols, anthocyanins, also exhibit significant free radical

scavenging and antioxidant activities [41]. Further investigations have revealed that anthocyanins can suppress cancer cell viability and induce apoptosis, thereby manifesting their anti-cancer effects [42].

TA, a weakly acidic polyphenol that includes digalloyl esters, is divided into hydrolysable and non-hydrolysable tannins [43]. As an important member of the natural polyphenol family, TA has a wide range of applications. Studies suggest that TA can protect megakaryocytes from apoptosis induced by ionizing radiation and inhibit changes in mitochondrial membrane potential by reducing the production of reactive oxygen species (ROS) [44]. In addition to its role in scavenging oxygen radicals, TA has been shown to suppress the growth of various cancers [45]. For instance, the Huang group discovered that TA inhibits bladder cancer cell proliferation by weakening the phosphorylation levels of Protein Kinase B [46]. Concerning lung cancer, it was found that TA could diminish the sphere-forming ability of lung cancer cells, influencing their stemness while simultaneously reducing the expression of cancer stem cell markers (SOX2, OCT4) [45]. Moreover, TA has a broad application in antimicrobial settings [47]. In this context, Sileika et al., has demonstrated

Table 1 The structure and application of classic natural polyphenols

| Polyphenols | Structure | Applications | Refs | Polyphenols | Structure | Applications | Refs |
|--------------------------|---|---|----------|-------------|--|--------------------------------|----------|
| Anthocyanin |  | Antioxidant Anti-cancer | [41, 42] | Gossypol |  | Anti-cancer | [60] |
| Epigallocatechin gallate |  | Antioxidant | [38] | TA |  | Antimicrobial Anti-cancer | [15, 46] |
| Resveratrol |  | Antimicrobial Periodontitis Anti-cancer | [53–55] | Quercetin |  | Cardioprotective Anticancer | [49–51] |
| Curcumin |  | Wound healing | [57] | Gallic acid |  | Anti-inflammation | [63] |

that polycarbonate surfaces modified with TA exhibit a strong bactericidal effect on *Staphylococcus aureus* and *Pseudomonas aeruginosa* [15].

Quercetin, a member of the natural polyphenol family, possesses various pharmacological functions such as antioxidant, anti-cancer, and anti-aging effects. Studies by Gao has found that quercetin can mitigate acute kidney injury by inhibiting ferroptosis through the reduction of malondialdehyde and lipid reactive oxygen levels [48]. In cancer therapy, quercetin has been reported to promote apoptosis in breast cancer cells and enhance their sensitivity to chemotherapy drugs like doxorubicin (DOX) [49, 50]. Notably, quercetin also exerts cardioprotective effects through inhibiting low-density lipoprotein oxidation, promoting vasodilation, and reducing the presence of adhesion molecules [51].

Resveratrol, a naturally potent antioxidant polyphenol, is an active component in the infamous "French paradox"—the observation that the French suffer a relatively low incidence of coronary heart disease despite a diet rich in high-fat foods and red wine [52]. Additionally, resveratrol has shown excellent antimicrobial activity, not only exhibiting antibacterial activity against a variety of bacteria but also enhancing the bactericidal capabilities of other antibiotics [53]. Other studies have found that resveratrol can inhibit lipopolysaccharide-mediated periodontal inflammation and activate antioxidant systems to prevent alveolar bone loss [54]. As an anti-cancer agent, resveratrol is also effective in various human cancers, inhibiting their growth [55]. For example, it is found that resveratrol suppresses the migration and invasion of colorectal cancer in vivo and in vitro by inhibiting TGF- β -induced epithelial-mesenchymal transition [56].

In addition to the polyphenols mentioned previously, natural polyphenols such as Curcumin, Gossypol, Hispolon, Ellagic acid (EA), gallic acid (GA), and others, have proven to be of great importance in the biomedical field due to their antioxidant, antimicrobial, and antitumor activities [57–63].

Artificial polyphenols

Despite the biological activities of natural polyphenols, such as their antioxidant and anti-tumor effects, their bioavailability and stability are rather unsatisfactory. The instability of natural polyphenols often influences their absorption and metabolic cycle, ultimately resulting in reduced bioavailability. Generally, only about 5–10% of natural polyphenols are absorbed in the small intestine, with the remainder being excreted with feces [64]. Additionally, the digestibility of natural polyphenols can affect their functional properties. For instance, polyphenols that are easily decomposed usually have a more significant effect during gastrointestinal digestion [65].

Given the limitations of natural polyphenols, synthetic polyphenols have become a focus of research. The main research directions for synthetic polyphenols include modification of polyphenols and the construction of composite polyphenolic components. Common covalent modification methods for polyphenols are hydroxylation, glycosylation and among others [66]. Both hydroxylation and glycosylation have been proven to effectively enhance the bioavailability and biological activity of polyphenols. The hydroxylation of polyphenols can yield various hydroxylated products depending on the reaction conditions (e.g., polyphenol oxidase, etc.) to obtain ortho-hydroxyphenols, or para-hydroxyphenols. In contrast, the synthesis of glycosylated polyphenols is typically achieved by coupling polyphenols with nucleotide di-phosphate (NDP)-sugars through metabolic engineering in modified cells [67].

Beyond various modifications of natural polyphenols, polyphenolic molecules can also be anchored onto various substances to form functional polyphenolic components. A common method involves the amide coupling reaction to combine polyphenolic compounds with polyethylene glycol (PEG) structures [68, 69]; Moreover, polyphenols can be conjugated with several natural macromolecules, such as hyaluronic acid and alginate [70]. Lastly, one research direction of functional polyphenolic components includes combining polyphenols with various chemotherapeutic drugs to enhance the biological distribution and efficacy of the medications. For example, the Messersmith research group conjugated the anti-cancer drug bortezomib with catechol for the specific targeting of tumors [71]. Although there are a variety of synthetic and modification methods for synthetic polyphenols, the principle remains to utilize the properties of polyphenols to enhance their bioavailability and biological activities.

Metal ions

Metal ions are not only essential trace elements required by the human body but are also increasingly being utilized in disease diagnosis and treatment. In terms of maintaining bodily functions, metal ions are involved in intercellular communication, maintaining electrical charges and osmotic pressure, electron transfer, and the regulation of DNA transcription and other fundamental physiological activities [72]. In the diagnosis and treatment of diseases, metal ions can exert different therapeutic effects based on their unique properties and may also impact the body due to their intrinsic systemic toxicity [73]. The application of metal ions in the field of nanomedicine is exceptionally broad, primarily encompassing tumor therapy, antimicrobial action, bone regeneration, and angiogenesis [30, 74–76].

Metal ions are crucial components of MPNs, including transition elements or lanthanide metals such as Fe^{III} , Al^{III} , Zn^{II} , Cu^{II} , and Ag^+ . Iron-based metal phenolic networks are one of the most common types and are currently used extensively in tumor-related research. Compared with other iron-based nano components, iron-based metal phenolic networks possess stronger catalytic abilities for Fenton reactions, releasing more hydroxyl radicals to efficiently kill tumor cells [77]. Besides iron-based MPNs, other metal-based MPNs (with metal ions like Cu^{II} , Mn^{II} , Ni^{II} , Gd^{II} , etc.) can also play various roles in nanomedicine [78].

The coordination of polyphenols and metal iron

Current research has revealed that within MPN, polyphenols can coordinate with metal ions in many ways, predominantly including Cation- π Interaction, Coordination Bonding, Redox Reaction, and Dynamic Covalent Bonding (Fig. 1) [79]. The Cation- π interaction was first discovered by Dougherty and others, who found that electron-rich π systems such as those in tyrosine and tryptophan can provide effective binding sites for alkaline metal ions [80]. This interaction occurs when

alkaline metal ions bind with the aromatic rings in polyphenols, and since Cation- π is a type of electrostatic interaction, the aromatic groups in polyphenols with different electron densities will affect the strength of the bond. Furthermore, the strength of Cation- π bonding with different metal ions varies; typically, the strength of the bonding with alkaline metal ions (Li^{II} , Na^{II} , K^{I}) is greater than that with transition metal ions (Ag^{II} and Cu^{II}) [81]. Another mode of interaction between metal ions and polyphenols is Coordination. This involves two or more polyphenolic ligands donating electron pairs to the vacant orbitals of metal ions to form a bond. In this bonding mode, the structure of the metal ions often determines the color of the MPN. Redox interactions are commonly seen with noble metal ions binding to polyphenols. Noble metal ions can oxidize the catechol part of polyphenols into semiquinone/quinone forms [82–84], and they can also be reduced to the metallic state by accepting electrons from polyphenols. The oxidized polyphenols can stabilize metal nanoparticles [85–87]. Dynamic Covalent Bonding is also a way for metal ions to bind with polyphenols. Metalloids, having both metallic and non-metallic physicochemical properties, with

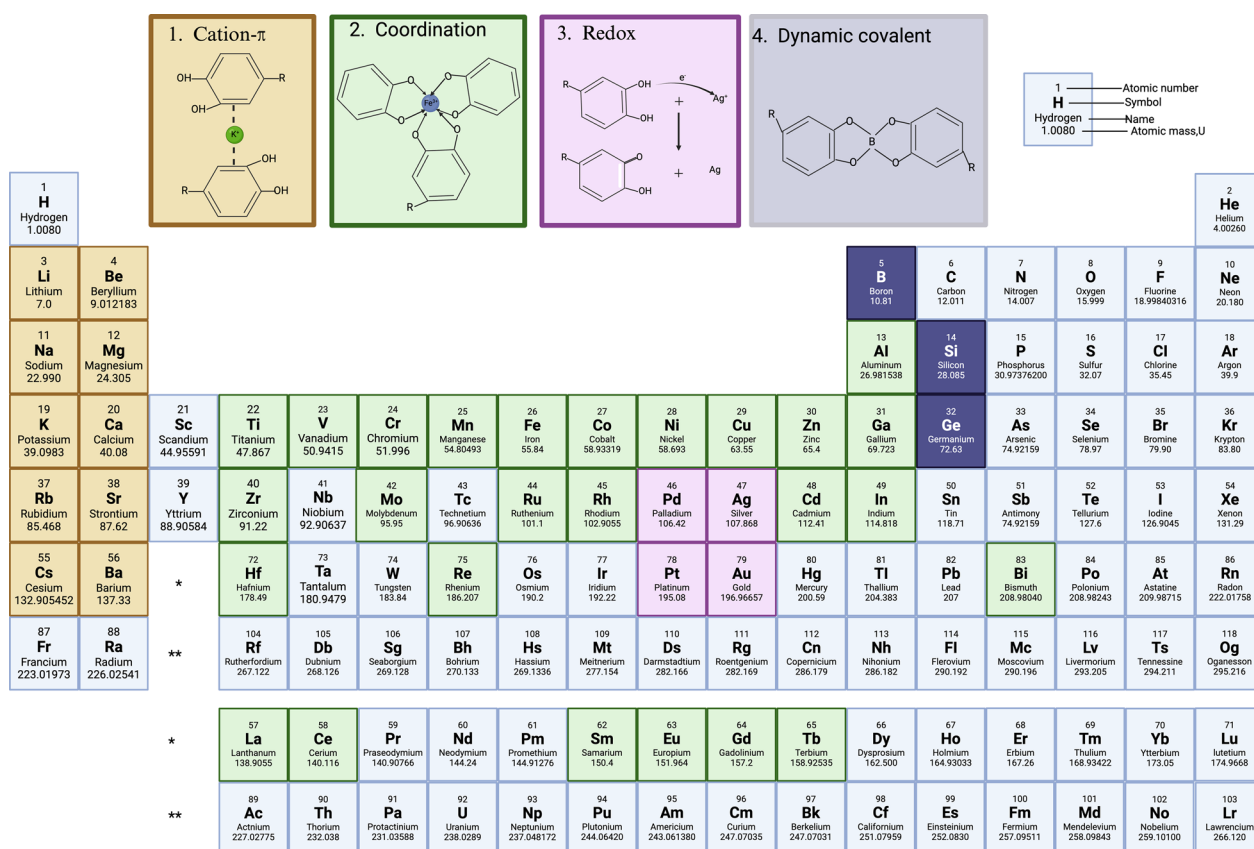


Fig. 1 The interaction methods between metal ions and polyphenol. Various colors represent distinct ways in which metal ions and polyphenols interact. This figure was drawn by biorender.com

typical elements being B, Si, etc., have been found by Hartmann and others to have a high affinity for phenolic compounds, with which they can form covalently bonded networks [88].

Owing to the high affinity of polyphenolic materials and the specific physicochemical functionalities of metal ions, MPNs can often form multifunctional nanoplat-forms on various interfaces [26, 89]. The properties and functionalities of MPNs formed by different metal ions and various polyphenolic substances also vary [90–95].

The fabrication methods of MPN

The synthesis of MPNs is characterized by its simplicity, speed, and environmental friendliness, when compared to the synthesis processes of other nanomaterials. The process of MPN assembly can be described as follows: By means of basic physical mixing, positively charged metal ions chelate with the electron-rich phenolic hydroxyl

groups found in polyphenols (the degree of this chelation is influenced by external factors, such as temperature, pH, etc.). Following chelation, the metal ions and polyphenols undergo spontaneous aggregation, resulting in the formation of particles with a wide range of sizes, spanning from nanometers to micrometers. This section provides a concise overview of various prevalent assembly methods employed for MPNs, elucidating their distinct procedures and advantages.

Direct self-assembly

The direct self-assembly of MPNs can be classified into one-step synthesis and multi-step synthesis methods (Fig. 2A) [18]. The one-step synthesis method is the most direct and commonly employed approach in the fabrication of MPNs. In 2013, Caruso et al., documented the successful assembly of MPNs using a one-step approach [19]. This involved combining TA with Fe^{III} ions in a

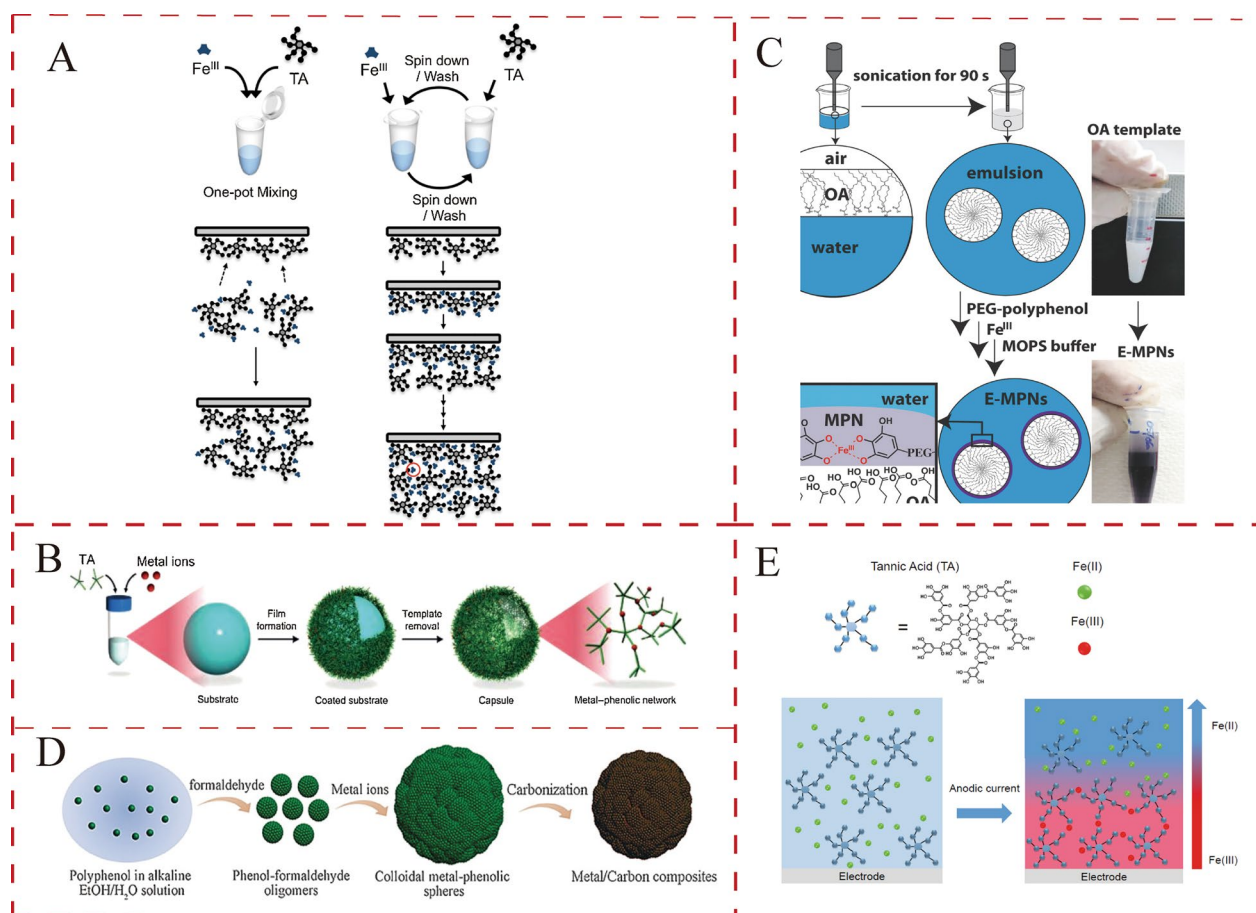


Fig. 2 The fabrication methods of the MPN. **A** Direct self-assembly of MPN. Reproduced with permission from Ref. [18]. Copyright 2017, Elsevier. **B** Templating assembly methods of MPN. Reproduced with permission from Ref. [105]. Copyright 2015, Wiley-VCH. **C** Emulsion-based self-assembly method of MPN. Reproduced with permission from Ref. [111]. Copyright 2018, Wiley-VCH. **D** Sol-gel assembly methods of MPN. Reproduced with permission from Ref. [114]. Copyright 2018, Wiley-VCH. **E** Electrically triggered assembly methods of MPN. Reproduced with permission from Ref. [115]. Copyright 2017, ACS

solution that contained a template. The process entails the adsorption of a fraction of TA molecules onto the surface of a polystyrene template, while another fraction undergoes a reaction with $\text{Fe}^{\text{III}+}$ to generate $\text{Fe}^{\text{III}+}$ -TA complexes. These complexes subsequently deposit onto the template, resulting in the formation of a layer with a thickness of approximately 10 nm. Owing to the intrinsically strong adhesion properties of polyphenols, various substances including polystyrene, mesoporous silica [96], CaCao3 [19], MOFs [97] and others, can function as substrates for the one-step method. Furthermore, the surface potential of the templates has no bearing on the self-assembly of metal ions with polyphenols, which eventually results in a negative surface potential. Thus, one-step synthesis of MPNs does not require specific solvents, complex equipment. In addition, the materials are readily available and inexpensive.

In addition to the one-step approach, multi-step self-assembly comprises a prevalent method used for the synthesis of MPNs [98, 99]. The underlying concept is that polyphenol ligands containing multiple hydroxyl groups can repetitively and alternately bind with metal ions to create multilayer MPN films. In this context, Rahim et al., synthesized MPNs by utilizing TA and $\text{Fe}^{\text{III}+}$ ions through a multi-step self-assembly approach [100]. During this process, excess TA molecules adsorbed onto the surface of the template. Subsequently, the unbound TA molecules were rinsed off, and an excess of $\text{Fe}^{\text{III}+}$ ions was introduced to initiate a cyclic self-assembly procedure. Finally, the process was completed through the repeated rinsing of the unabsorbed polyphenol molecules and metal ions, followed by the addition of fresh polyphenols and metal ions in each cycle. A key advantage of the multi-step approach is its ability to regulate the thickness of the MPN, which typically increases with an increase in the pH level of the solution. Accordingly, Guo et al., employed TA, a natural polyphenol, along with various metal ions to create a collection of MPN capsules with functional properties [101]. Herein, the choice of metal ions was used to modulate the functional properties of the MPN capsules, such as drug delivery, fluorescence behavior, catalysis, etc., as well as their thickness. As a result, MPNs generated through multi-step assembly exhibit an increased concentration of metal ions. Considering these attributes, the multi-step self-assembly approach presents substantial potential applications in the fields of materials science and nanomedicine. Accordingly, Caruso et al., and other researchers explored the interaction between rusty iron nails and solutions containing GA, demonstrating that GA has the ability to etch iron from rust layers and form stable MPN coatings by chelating with it [102]. Furthermore, the findings of the study revealed a dual dynamic process, involving both

etching and self-assembly of MPNs, thus offering novel insights on the utilization of MPNs in the field of materials science.

Templating assembly

Template-mediated synthesis comprises another frequently employed approach for the fabrication of MPNs. Due to the strong adhesive properties of polyphenols, they can be easily deposited onto different template surfaces for the purpose of assembly and synthesis of MPNs. The template-mediated assembly process of MPNs typically involves two primary steps: (1) Synthesis of the metal-phenolic network on the template surface, and (2) Removal of the template material. Correspondingly, template-mediated assembly can yield MPNs with diverse morphologies and functionalities by using various templates, including two-dimensional materials, nanoparticles, vesicles, and nanosheets [103]. CaCO_3 comprises one of the most commonly used substrates for the template-mediated assembly of MPNs due to its facile synthesis route, controllable size and shape, and ease of removal [104]. In this context, Caruso et al., first used CaCO_3 as a template for the in-situ fabrication of an $\text{Al}^{\text{III}+}$ -TA MPN film at a pH of 8 (Fig. 2B) [105]. By removing the substrate template, they successfully produced pH responsive MPN capsules for the delivery of anticancer drugs. In addition to CaCO_3 , other materials have also been used in the template-mediated fabrication of MPNs. Accordingly, Feng et al., have shown that the combination of TA and $\text{Fe}^{\text{III}+}$ can yield uniform nanocoating on the surfaces of templates like poly(lactic-co-glycolic acid) (PLGA) and mesoporous silica nanoparticles (MSN) [78]. In addition, Yan et al., designed $\text{Fe}^{\text{III}+}$ and TA assemblies on the surface of paclitaxel nanoparticles, resulting in a uniform metal-phenolic coating. Subsequently, when the substrate was removed, capsule structures were formed, which were capable of delivering anticancer drugs [106]. In addition to producing films and capsule structures, the template-mediated method can also be employed for the synthesis of MPN nanoparticles [107]. In this context, Caruso et al., achieved the synthesis of MPN nanoparticles with an ordered mesoporous configuration by employing polymer cubes as templates possessing a comparable mesoporous structure [108]. These MPN nanoparticles exhibited significantly greater porosity compared to MPN films, making them particularly advantageous for drug delivery applications in nanomedicine.

Emulsion-based self-assembly

Emulsion-based self-assembly comprises another notable technique for synthesizing MPNs. An emulsion is a blend of two immiscible liquids, such as water and oil,

enabling it to dissolve drugs that are both hydrophilic and hydrophobic in nature [109]. The immiscible liquids in an emulsion create a physical barrier that stops the droplets from coalescing, thus ensuring stability. Emulsions, in comparison to other templates utilized in synthesis, provide superior biocompatibility and drug loading capabilities [110]. The primary techniques used for synthesizing emulsions encompass high-pressure methods, ultrasonication, phase inversion temperature, and homogenization. Emulsion-based MPN self-assembly can be classified into two categories: self-assembly at various liquid interfaces of the emulsion and self-assembly within the emulsion itself. In this context, Caruso et al., employed a water-in-oil emulsion as a template to spontaneously form pH-responsive MPN coatings at their interface (Fig. 2C) [111]. In their research, they first generated emulsions with diameters ranging from 100 to 250 nm through the process of ultrasonication. Subsequently, by utilizing the emulsion as a template, they synthesized interfacial MPNs that demonstrated enhanced stability and pH responsiveness. The findings demonstrated that the utilization of these MPN-coated emulsions for administering anticancer drugs resulted in heightened therapeutic efficacy. Furthermore, Liang et al., conducted additional investigations to examine the impact of various MPN structures on the stability of emulsions [112]. The resultant findings revealed that the level of polyphenols and the proportion of polyphenols to metal ions had an impact on the interfacial characteristics and the stability of the emulsion. More precisely, higher concentrations of polyphenols and extensive crosslinking between metals and polyphenols led to enhanced stability of the emulsion.

Furthermore, MPNs can be constructed directly within the emulsion, in addition to the necessary interface preparation. In this context, Dai et al., investigated the process of self-assembly of polyphenol-functionalized drugs and metal ions in an emulsion, resulting in the formation of MPN nanoparticles with a diameter of approximately 100 nm [113]. The as-obtained MPN nanoparticles demonstrated high drug loading capacity and low toxicity, showing promising anti-tumor efficacy in combating prostate cancer in mouse models.

Other assembly methods

The sol–gel synthesis technique comprises one of the other approaches that has been commonly utilized for the fabrication of MPNs, frequently involving the use of formaldehyde (Fig. 2D) [114]. A characteristic of the sol–gel synthesis approach is the facile, template-free synthesis of MPNs. During the sol–gel synthesis method, polyphenols initially undergo pre-crosslinking with formaldehyde in an alkaline solution, resulting in

the formation of phenolic polymers. Subsequently, various metal ions (mono-metal, bi-metal, or multi-metal) are introduced into the solution containing the phenolic polymers to crosslink and generate MPN nanospheres. These MPN nanospheres, synthesized using the sol–gel technique, subsequently serve as precursors for electrodes that exhibit excellent electrocatalytic properties.

In addition to the above, there are synthesis methods for MPNs that necessitate specific external stimuli. Of these approaches, electrically triggered assembly comprises a process in which metal ions dissolve and spread in a solution under the influence of an electric field. This occurs through an anodic process, resulting in the formation of a gradient film on the surface of a substrate template. Accordingly, Boulmedais et al., successfully synthesized $\text{Fe}^{\text{III+}}$ -TA MPN nanocoatings through an electrically induced self-assembly approach involving a combination of TA and $\text{Fe}^{\text{II+}}$ ions (Fig. 2E) [115]. When the electrode met the $\text{Fe}^{\text{II+}}$ ions and a current was applied to the anode, these $\text{Fe}^{\text{II+}}$ ions underwent oxidation to $\text{Fe}^{\text{III+}}$ ions, resulting in the localized formation of $\text{Fe}^{\text{III+}}$ -TA MPNs. In addition, the thickness and assembly kinetics of these MPN nanocoatings could be controlled by manipulating the molar ratio of $\text{Fe}^{\text{II+}}$ /TA, the current intensity, and the duration of electrical stimulation. As a result, this electrically triggered approach offers novel avenues for employing MPNs as protective coatings with antioxidant properties.

The properties of MPN

The composition of MPNs includes both polyphenols and metal ions, resulting in a high abundance of functional characteristics. The functional characteristics of the MPNs are influenced by the specific type of polyphenol and metal ion. In general, the distinct properties of MPNs depend on the selection of different metal ions and polyphenols (Table 2). Therefore, it is crucial to classify and summarize these diverse functionalities.

Adhesive property

Numerous polyphenols contain pyrogallol chemical structures, which frequently confer them with exceptional interfacial adhesion properties [116]. By utilizing this attribute, MPNs can stick to various substrates, such as biological surfaces, and offer specific functionalities [117, 118]. This binding affinity of polyphenols is largely attributed to noncovalent interactions, including electrostatic interactions, hydrogen bonding, π – π stacking, hydrophobic interactions, and van der Waals forces [119]. For example, the binding ability of polyphenols to proteins, RNA, DNA, and small molecules is facilitated through these noncovalent interactions. Consequently, the adhesive properties of MPNs can be

Table 2 The structure and properties of MPNs based on different metal ions and polyphenols

| Metal | Polyphenol | Structure | Properties | Refs |
|---------------------|----------------|--|-----------------------------|-------|
| Fe ^{III+} | EGCG | Fe ^{III+} -EGCG emulsion | Stability | [112] |
| Fe ^{III+} | Myricetrin | Fe ^{III+} -myricetrin film | Antioxidant | [244] |
| Fe ^{III+} | TA | Fe ^{III+} -TA hydrogel | Adhesiveness; Photothermal | [175] |
| Fe ^{III+} | TA | Fe ^{III+} -TA film | PH responsiveness | [19] |
| Fe ^{III+} | TA | Fe ^{III+} -TA particle | Photothermal and imaging | [78] |
| V ^{III+} | TA | V ^{III+} -TA particle | Photothermal and imaging | [78] |
| Ru ^{III+} | TA | Ru ^{III+} -TA particle | Photothermal and imaging | [78] |
| Fe ^{III+} | TA | SRF@Fe ^{III+} TA NPs | Ferroptosis; Photodynamic | [77] |
| Fe ^{III+} | TA | GOx@ZIF@MPN | Inducing Fenton reaction | [97] |
| Fe ^{III+} | GA | Fe ^{III+} -GA Film | Controllable thickness | [102] |
| Fe ^{III+} | HA and PEG | MPN-HA-PEG capsules | Specific targeting | [104] |
| Al ^{III+} | TA | Al ^{III+} -TA Capsules | Ph-responsive | [105] |
| Fe ^{III+} | TA | PTX@Fe ^{III+} -TA NPs | Long-term stability | [106] |
| Fe ^{III+} | Peg-polyphenol | Fe ^{III+} -PEG-DOX NPS | Ph-responsive | [111] |
| Fe ^{III+} | Pt-polyphenol | Fe ^{III+} -PEG-Pt NPS | long circulation times | [113] |
| Co ^{II+} | TA | Co ^{II+} -TA sphere | Electrocatalytic | [114] |
| Fe ^{III+} | TA | Fe ^{III+} -TA coating | Antioxidant | [115] |
| Eu ^{II+} | TA | Zein/HTCC-TA/ NPs | Ph-responsive; Imaging | [118] |
| Fe ^{III+} | TA | Fe ^{III+} -TA Shell | Degrades on-demand | [122] |
| Fe ^{III+} | TA | Fe ^{III+} -TA Coating | Stimu-responsive | [112] |
| Fe ^{III+} | EA | Fe ^{III+} -EA NPs | Photothermal | [133] |
| Fe ^{III+} | Anthocyanins | Fe ^{III+} -A-P NPs | Dual imaging; photothermal | [118] |
| Fe ^{III+} | TA | Fe ^{III+} -TA@MSN NPs | Endosomal escape | [145] |
| Fe ^{II+} | gossypol | PEG-Ce6-Fe ^{II+} -gossypol | Photodynamic | [153] |
| Fe ^{II+} | Quercetin | Qu- Fe ^{II+} P | Photothermal | [156] |
| Hf ^{IV+} | GA; PEG; Ce6 | Hb@Hf-Ce6 NPs | Improve the hypoxic | [159] |
| Gd ^{III+} | TA | AuNR@MSN@MON | Photothermal | [107] |
| Mg ^{II+} | EGCG | Mg ^{II+} -EGCG MPN | Light-responsive | [173] |
| Re ^{III+} | Catechin | Re ^{III+} -Cat NPs | Antibacterial | [174] |
| Cu ^{II+} | EGCG | Cu ^{II+} -EGCG nanosheet | ROS scavenging | [177] |
| Sr ^{II+} | TA | Sr ^{II+} -TA coating | Eliminate cytokines/ROS | [178] |
| Zinc ^{II+} | Kaempferol | Zinc ^{II+} - Kaemferal | Promoting bone growth | [181] |
| Fe ^{II+} | GA | Fe ^{II+} -GA NPs | Photothermal; increase ROS | [188] |
| Co ^{III+} | TA | Cobalt ^{III+} -TA @gold | Inhibited amyloid formation | [197] |
| Mg ^{II+} | TA | Mg ^{II+} -TA Film | Osteocompatibility | [201] |
| Ti ^{IV+} | TA | Ti ^{IV+} -TA gelation | Biocompatibility | [204] |
| Zn ^{II+} | TA | Fe ₃ O ₄ -NH ₂ -(TA-Zn ^{II+}) | Magnetic | [90] |
| Cu ^{II+} | TA | Cu ^{II+} -TA coating | Antimicrobial | [256] |
| Cu ^{II+} | DA | Cu ^{II+} -DA coating | Antimicrobial | [256] |
| Cu ^{II+} | Norepinephrine | Cu ^{II+} -Ne coating | Antimicrobial | [256] |
| Mn ^{II+} | TA | Mn ^{II+} -TA @BPNSs | Photothermal and imaging | [91] |
| Ru ^{III+} | TA | Ru ^{III+} -TA Capsules | Stimuli-responsiveness | [101] |
| Rh ^{III+} | TA | Rh ^{III+} -TA Capsules | Stimuli-responsiveness | [101] |
| Ce ^{III+} | TA | Ce ^{III+} -TA Capsules | Stimuli-responsiveness | [101] |
| Cr ^{III+} | TA | Cr ^{III+} -TA Capsules | Stimuli-responsiveness | [101] |
| Cd ^{II+} | TA | Cd ^{II+} -TA Capsules | Stimuli-responsiveness | [101] |
| Tb ^{III+} | TA | Tb ^{III+} -TA Capsules | Stimuli-responsiveness | [101] |
| Zr ^{IV+} | TA | Zr ^{IV+} -TA Capsules | Stimuli-responsiveness | [101] |
| Mo ^{II+} | TA | Mo ^{II+} -TA Capsules | Stimuli-responsiveness | [101] |

Table 2 (continued)

| Metal | Polyphenol | Structure | Properties | Refs |
|--------------------|----------------|---------------------------------------|--|-------|
| Ti ^{IV+} | TA | Ti ^{IV+} -TA metallogel | Robustness and flexibility | [148] |
| Mn ^{II+} | TA | Mn ^{II+} -TA complex | Photothermal conversion | [163] |
| Fe ^{III+} | Lignin | Fe ^{III+} -Lignin Capsules | Stability; high drug loading | [92] |
| Fe ^{III+} | ACN | ACN-Fe ^{III+} -PLG-g-mPEG | Photothermal and imaging | [134] |
| Fe ^{III+} | Luteolin | Fe ^{III+} -Luteolin Capsules | ROS scavenging | [93] |
| Fe ^{III+} | Fisetin | Fe ^{III+} -Fisetin Capsules | ROS scavenging | [93] |
| Pt ^{II+} | EGCG | Pt ^{II+} -EGCG NPs | Stability; high drug loading | [213] |
| Fe ^{III+} | PG | Fe ^{III+} -PG Capsules | High loading capability | [95] |
| Fe ^{III+} | PC | Fe ^{III+} -PC Capsules | High loading capability | [95] |
| Ti ^{IV+} | Proanthocyanin | Ti ^{IV+} -PAC NPs | Anti- biofilm formation | [170] |
| Fe ^{III+} | Shikonin | Fe ^{III+} -Sk-PEG/cRGD | Induce ferroptosis | [164] |
| Cu ^{II+} | GA | CS-Cu ^{II+} -GA NCs | Facilitate production of H ₂ O ₂ | [171] |

tailored by selecting different polyphenols. Natural polyphenols, such as TA, pyrogallol, and EGCG, have demonstrated strong adhesive properties. Consequently, the remarkable adhesive properties of MPNs can synergistically integrate the functionalities of the MPNs with the derivative functions of substrates for optimal efficacy. For instance, Li et al., developed pH-responsive drug-delivery nanoparticles measuring 100–200 nm in size by attaching Eu^{III+}-TA MPNs to zein/quaternized chitosan (HTCC) nanoparticles [120]. Furthermore, MPNs can be deposited on two-dimensional materials to create nanomaterials with novel functions. In this context, Haga et al., employed Fe-TA MPNs to bind to graphene oxide nanosheets (GO), yielding novel nanosheets that exhibited improved dispersibility and stability in water [121]. Due to the exceptional biocompatibility of MPNs, they can also be attached to biological surfaces. For example, Park et al., utilized a layer of Fe^{III+}-TA MPN to coat the surface of yeast cells, providing protection against ultraviolet (UV) damage [122].

Stimuli-responsive property

One notable characteristic of MPNs is their ability to react to different external factors, including pH, glutathione (GSH), adenosine triphosphate (ATP), redox potentials, etc. [123]. MPNs often exhibit stimuli-responsive properties due to the stimuli-sensitive coordination between the catechol groups in polyphenols and metal ions. The stimuli-responsiveness of MPNs is influenced by the type, valence state, and composition ratio of metal ions [124, 125]. For the same metal ion, different polyphenols exhibit varying chelation abilities [124]. Additionally, the chelation ability differs between different valence states of the same metal ion. Furthermore, high-valence metal ions such as Zr^{IV+} and Fe^{III+} generally have stronger chelation abilities with polyphenols than

lower-valence ions like Cu^{II+} and Fe^{II+}. The composition ratio of metals and polyphenols in MPNs also affects their acid-sensitive responsiveness. Overall, the acid sensitivity of MPNs decreases as the metal content increases, due to higher coordination degrees that enhance system stability, thereby reducing acid sensitivity [120]. Based on these characteristics, appropriate polyphenols, metals, and control of the metal-to-polyphenol ratio can be selected to design MPNs suitable for drug-controlled release according to specific needs. Given the variation in pH levels in different biological microenvironments—such as the Tumor Microenvironment (TME) with a pH range of 5.7–6.8, and lysosomes with a pH range of 4.5–5.0—MPNs are ideal for the development of targeted drug delivery systems. In this context, Ping et al., as well as other researchers have utilized Al^{III+}-TA MPN capsules to encapsulate the anticancer drug DOX for the purpose of treating tumors. Accordingly, the Al^{III+}-TA MPN-based nanocarrier platform was found to demonstrate an increased drug loading capacity and pH-responsive release in the acidic tumor environment [105].

Furthermore, in order to cater to the diverse range of uses of MPNs in nanomedicine, MPNs have been engineered to possess multiple responsive attributes, such as reactions to GSH, ROS, ATP, etc. GSH, which comprises a reductive substance, is overexpressed in cancer cells [126]. The GSH-responsive characteristic of MPNs primarily relies on the ability of GSH to convert Fe^{III+} in Fe^{III+}-based MPNs to Fe^{II+}, leading to the disintegration of the MPN. In this context, Du et al., have reported the encapsulation of an Fe^{III+}-TA network within a MOF to produce nanoparticles with the ability to release drugs in response to seven distinct stimuli, also including near-infrared light, H₂O₂ and so on [127]. The aforementioned seven stimuli primarily pertained to physiological processes and the natural environment, encompassing

glutathione. Moreover, ROS, which play a crucial role in normal physiological processes and cancer therapy, have been gaining increasing attention in the development and design of MPNs [128]. Accordingly, Shi et al., have reported the development of ROS-responsive nanocomposites for the treatment of tumors by enclosing poly(amidoamine) dendrimers and the drug toyocamycin within an Fe^{III} -TA network [129]. It is also worth mentioning that ATP, which is frequently increased in pathological states, has led to the exploration of ATP-responsive MPNs as a promising avenue for research. In this context, Zhang et al., reported the synthesis of an ATP-responsive self-catalyzed Fenton nanosystem (GOx@ZIF@MPN). Owing to the abnormally high levels of ATP in cancer cells, the MPN shell of the GOx@ZIF@MPN easily disintegrated, leading to the release of the internal drugs to effectively eliminate the tumor [97].

Photothermal property

Nanomaterials possessing photothermal properties have consistently been a central focus in the realm of nanomedicine. Currently, nanomaterials intended for photothermal conversion exhibit several drawbacks, including complex synthesis procedures, low photothermal conversion efficiency, and limited drug loading capacity. MPNs, exhibit excellent ligand-to-metal conversion properties, resulting in their remarkable UV-vis- near-infrared (NIR) absorption capabilities when exposed to near-infrared light. Additionally, as a result of plasma resonance and energy conversion properties, MPNs have the ability to transform absorbed light into thermal energy [130]. The NIR absorption ability of MPNs can be adjusted by manipulating the coordination ligands, as the d-d electronic transitions of metal ions are highly dependent on the properties of the ligands. For example, polyphenols with more catechol groups can coordinate with a greater number of iron ions. In summary, a high iron content combined with a small particle diameter enhances photothermal performance. Among the MPNs with photothermal properties, TA based MPNs is the most encountered variants. Compared to other photothermal conversion nanomaterials, TA based MPNs present advantages such as eco-friendly synthesis, facile binding with metal ions, strong adherence properties, and high photothermal conversion rates. Research conducted by Feng et al. revealed that TA based MPNs containing Fe^{III} , V^{III} , and Ru^{III} exhibit exceptionally high photothermal conversion efficiencies ($\eta \approx 40\%$) [78], surpassing those of other commonly used photothermal materials such as gold nanorods (21%), $\text{Cu}_2\text{-xSe}$ (22%), and Cu_9S_5 (25.7%) [131, 132]. Furthermore, additional investigations by Feng et al., also indicated that an increase in the molar ratio of metal ions to TA

enhances the near-infrared absorption (650–1350 nm); Consequently, the photothermal conversion capacity of TA based MPNs are enhanced. In addition, the photothermal efficiency of TA-based MPNs were found to be independent of the type, structure of the substrate template or the or thickness of TA-based MPN itself [78]. In addition to TA based MPNs, MPNs utilizing alternative polyphenols such as EGCG, EA, GA, and QU have also exhibited favorable photothermal characteristics [133, 134]. As observed, the remarkable photothermal performance of MPNs forms the basis for their use in the field of nanomedicine.

Fenton reaction-inducing property

The Fenton and Fenton-like reactions involve the catalytic decomposition of hydrogen peroxide (H_2O_2) into ROS in the presence of metal ions. Correspondingly, the Fenton reaction can be represented by the following chemical equation: $\text{Fe}^{2+} + \text{H}_2\text{O}_2 \rightarrow \text{Fe}^{3+} + \cdot\text{OH} + \text{OH}^-$ [135]. As excessive ROS can induce oxidative stress damage in cells, Fenton and Fenton-like reactions are commonly used in the treatment of tumors and antimicrobial therapy [136]. However, the major obstacle in the implementation of the Fenton reaction lies in the limited catalytic efficacy of the initiating agents. This phenomenon is primarily attributed to the transformation of Fe^{II} ions into Fe^{III} ions during the catalytic process, wherein Fe^{III} ions have a lower catalytic efficiency in comparison to the Fe^{II} [137]. MPNs, due to their exceptionally high metal ion content, have the ability to initiate Fenton and Fenton-like reactions. Furthermore, the strong ability of polyphenols in MPNs to reduce Fe^{III} to Fe^{II} after catalysis helps in maintaining a higher level of catalytic performance [138]. Therefore, the higher the metal ion content in MPNs, the stronger their Fenton reaction-inducing properties. Accordingly, studies by Zhang et al., show that Fe^{III} -TA MPN efficiently converts Fe^{III} to Fe^{II} within 30 min, thereby catalyzing the Fenton reaction to produce a vast array of ROS [97]. In addition to the above, MPNs have the advantage of efficiently and selectively releasing metal ions to catalyze the Fenton reaction [139]. Moreover, MPNs not only trigger the Fenton reaction but also effectively catalyze Fenton-like reactions. In this context, a study conducted by Chen et al., revealed that Cu^{II} -TA MPN can catalyze the decomposition of H_2O_2 through a Fenton-like reaction, resulting in the production of a large amount of ROS and exhibiting an antitumor effect [140]. To summarize, MPNs demonstrate a high level of effectiveness in inducing Fenton and Fenton-like reactions, while also possessing numerous distinct catalytic benefits when compared to traditional catalysts.

Internalization and endo/lysosomal escape

Efficient uptake of nanomedicines by receptor cells and their precise transportation to specific locations while maintaining their functionality is a crucial prerequisite for achieving therapeutic outcomes [141]. Due to their small particle sizes, nanomaterials are readily internalized by cells through endocytosis. After being absorbed by cells, nanomaterials first enter early endosomes with a pH of 6.3; as the pH decreases over time, the endosomes develop into late endosomes, which eventually merge with lysosomes (pH 4–5) that contain hydrolytic enzymes [142]. This process serves as the central segment in vesicular trafficking and is known as the endosome-lysosome transport. During this transport, the surface structures of nanomaterials are prone to degradation by the lysosomal enzymes, leading to loss of activity, which significantly impacts their function and efficacy. Therefore, enhancing cellular uptake and facilitating endosome-lysosome escape to retain bioactivity is crucial for nanomaterials. MPNs, as a type of small nanoparticle, are often successfully internalized by cells [106]. Moreover, the MPN coating functions as a "proton sponge," which facilitates endosome/lysosome escape to preserve biological functionality (Fig. 3A). This "proton sponge" effect occurs when the nanomaterial undergoes protonation in the

acidic environment of the cellular endosomal vesicle, thereby modifying the vesicle's osmotic pressure. In addition, the acid ATPase enzymes present in the endosome/lysosome efficiently move protons from the cytoplasm to the vesicle, resulting in a substantial buffering capacity. Over time, the concomitant influx of protons, chloride ions, and water results in a higher osmotic pressure inside the vesicles, which eventually leads to the rupture of the vesicular membrane. This buffering capacity is essential for the nanomaterial to evade the endosome/lysosome, thereby resulting in the proton sponge effect, which destabilizes the membrane of the endosome/lysosome in an acidic environment [143, 144]. In this context, Caruso et al., conducted co-localization experiments within cells, and discovered that the localization of Fe^{III} -TA-coated MSN within endosomes/lysosomes was significantly reduced in comparison to bare MSNs, thus indicating that Fe^{III} -TA-coated MSN successfully evaded endosomes/lysosomes (Fig. 3B) [145]. The mechanism underlying the endosomal escape of NP@MPN involves NP@TA/ Fe^{III} , which induces osmotic swelling and subsequent rupture of endosomal/lysosomal membranes through the activation of the 'proton-sponge effect' (Fig. 3C). In addition, substituting the coordinated metal in the MPN with Al^{III} instead of Fe^{III} still enabled the

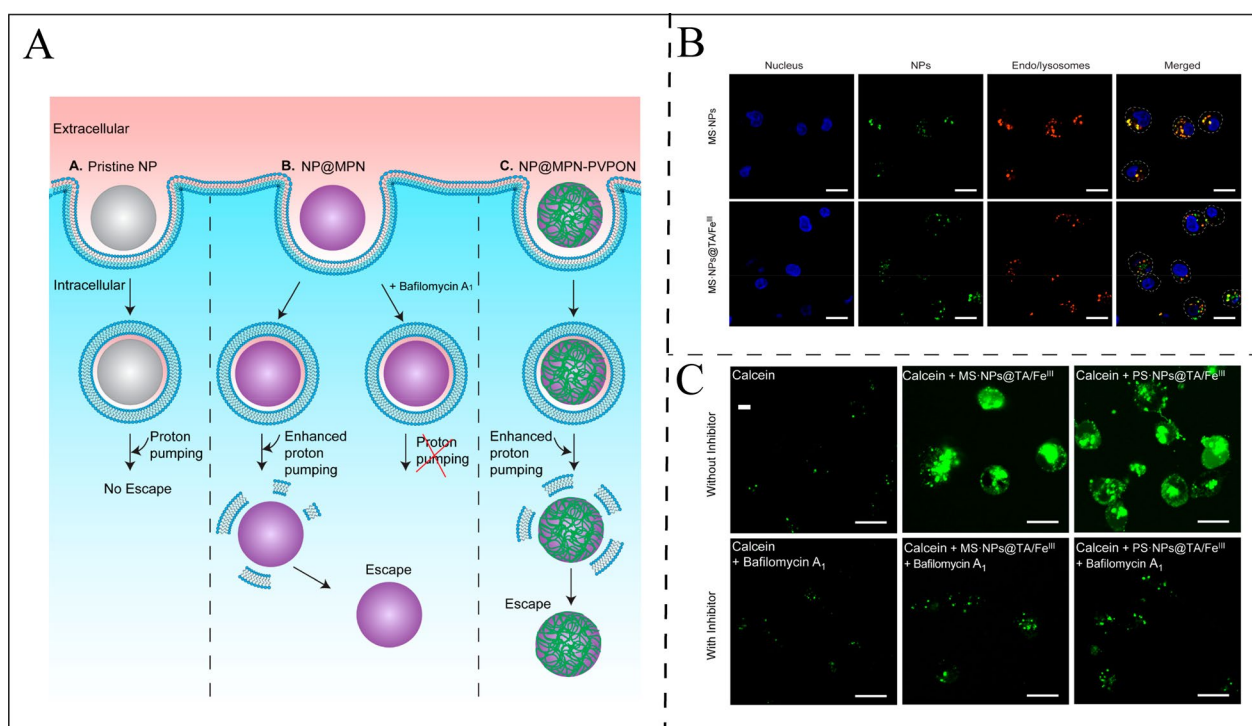


Fig. 3 The endosomal escape prosperity of MPNs. **A** The schematic illustration of MPNs Facilitate Endosomal Escape via the "Proton-Sponge Effect". **B** The confocal laser scanning microscopy (CLSM) images of the colocalization of MS-NP and MS-NPs@TA/ Fe^{III} in endo/lysosomes. **C** The CLSM images of cells incubated with calcein and NPs@TA/ Fe^{III} . Reproduced with permission from Ref. [145]. Copyright 2019, ACS

MPN to escape from endosomes/lysosomes. These findings, therefore, indicate that cells can effectively internalize both Fe-based MPNs and Al-based MPNs and evade endosomes/lysosomes, rendering them highly effective nanocarriers for drug delivery.

In situ gel-forming

MPNs also possess the ability to assemble into supramolecular hydrogels (commonly referred to as metal-phenolic gels). Unlike traditional gels, metal-phenolic based hydrogels can be formed by rapidly inducing non-covalent gelation between phenolic compounds or phenolic-modified polymers and metal ions [31]. Specifically, TA and transition metals are commonly chosen for the fabrication of metal-phenolic-based hydrogels. As a result, this process does not require the prior synthesis of large molecular building blocks, which is typically necessary for traditional gels. In this context, a series of metal-phenolic gels synthesized by Zhao et al., including single-metal, dual-metal, and multi-metal gels, have consistently demonstrated exceptional physicochemical properties, such as transparency and injectability [114]. In addition, the combination of polyethylene glycol-functionalized catechol groups (PEG-catechol) and Fe^{III} ions has been frequently employed to create metal-phenolic network hydrogel [146]. Expanding on this, Li et al., substituted Fe^{III} with Fe_3O_4 , resulting in the formation of a reversible hydrogel with the PEG-catechol moiety through metal coordination bonds [147]. The unique mechanical properties of this metal-phenolic gel were attributed from the dynamic formation of a supramolecular cross-linked structure. Unlike conventional transient fluid dynamics of catechol- Fe^{III} linkages, the catechol- Fe_3O_4 structure exhibited solid-like but reversible hydrogel mechanics.

In addition, Caruso et al., investigated the functionalities and applications of metal-phenolic gels created by combining TA with a range of group IV metals [148]. Initially, Ta and Ti^{IV} were selected to create a metal-phenolic gel that possesses optical transparency, moldability, shape persistence, adhesiveness, and high stability within a pH range of 2–10. The degradation of the TA- Ti^{IV} hydrogel commenced only when the pH of the surrounding environment surpassed 10. Moreover, in vitro assays revealed that the TA- Ti^{IV} hydrogel exhibited no toxicity to cells and was compatible with various surrounding mediums. Another advantage of the TA- Ti^{IV} hydrogel is its ability to incorporate different functional materials into the gel matrix through in-situ co-gelation, resulting in the formation of composite hydrogel materials. As observed, the numerous distinctive characteristics of MPN gels indicate that they are a highly promising form of hydrogel with significant potential.

The application of MPN based nanoplatform in nanomedicine

Due to the remarkable capabilities of MPNs, their use in the field of nanomedicine has become notably extensive. The inherent stability and responsiveness of MPNs make them suitable for use in cancer therapy. In addition, the photothermal properties of MPNs, combined with the intrinsic characteristics of the metal ions, enhance their potential in antimicrobial research and applications. Furthermore, the adhesive nature and reduction potential of the phenolic molecules in MPNs enable the formation of diverse composite nanomaterials, while the imaging capabilities of the metal ions in MPNs enhance their usefulness in biomedical imaging applications. In light of these factors, the current section presents a comprehensive overview of the applications and progress in research of MPN-based nanoplatforms in different areas of nanomedicine.

Cancer therapy

The varied attributes of MPNs indicate their potential as composite nanoplatforms for tumor-related therapies. Currently, MPN applications in tumor therapy can be categorized into several groups: Direct anticancer agents, Chemotherapy, Chemodynamic therapy (CDT), Photodynamic therapy (PDT), Photothermal therapy (PTT), TME-modulation therapy, and Multimodal combination therapy. In various cancer treatment strategies, MPNs primarily serve as carriers for the delivery of inducers in chemotherapy, PDT, some TME modulation therapies, and combination therapies. In other therapeutic approaches, MPNs function as the key active component.

Chemotherapy

Chemotherapy is the administration of different medications to eliminate cancer cells and is a widely used approach in the treatment of tumors. However, despite its widespread use in tumor therapy, chemotherapy still has several limitations, including low bioavailability of drugs, toxic side effects of drugs, and drug resistance [149]. The utilization of MPNs in chemotherapy primarily serving as nano-scale vehicles for the delivery of anti-cancer medications.

Furthermore, hollow MPN capsules have the potential to serve as highly effective nano-drug carriers for tumor chemotherapy. MPNs can remain stable for a long time in a pH range of 7–8, which contributes to their long-term stability during extended periods of blood circulation. However, upon entering the acidic tumor environment, MPNs undergo decomposition, thereby achieving targeted drug release. This is further validated from the study conducted by Caruso et al., reporting

the effective encapsulation of the anticancer drug DOX within $\text{Al}^{\text{III}+}$ -TA MPN capsules that were assembled utilizing CaCO_3 as a template. The findings show that the drug loaded MPN capsule demonstrated a high drug loading rate, responsiveness to pH, and effective ability to kill tumors [105].

Chemodynamic therapy and photodynamic therapy

Chemodynamic therapy and photodynamic therapy function by producing a significant quantity of ROS to eliminate cancerous cells. Chemodynamic therapy operates by inducing oxidative stress in cells and achieving antitumor effects through the utilization of metal ions via Fenton and Fenton-like reactions. Previous studies indicate that MPNs can trigger apoptosis in cancer cells by generating hydroxyl radicals via the Fenton reaction, which involves the liberation of metal ions such as $\text{Fe}^{\text{II}+}$, $\text{Cu}^{\text{II}+}$, $\text{Mn}^{\text{II}+}$, $\text{Ni}^{\text{II}+}$, and $\text{Co}^{\text{II}+}$ [150]. Accordingly, Liu et al., developed composite nanoparticles ($\text{CaO}_2@\text{ZIF8}@\text{MPN}$) consisting of CaO_2 enclosed in ZIF-8 and $\text{Fe}^{\text{III}+}$ -TA MPN assembled on the surface, that had the ability to generate H_2O_2 and recycle iron ions, thus enhancing CDT [151]. The findings show that the $\text{Fe}^{\text{III}+}$ -TA MPN coating on the $\text{CaO}_2@\text{ZIF8}@\text{MPN}$ decomposed in an acidic environment, subsequently undergoing Fenton reaction to generate ROS and inducing tumor cell death. Notably, CaO_2 could be broken down into H_2O_2 and $\text{Ca}^{\text{II}+}$, thus continuously providing sufficient substrates for CDT.

On the other hand, photodynamic therapy comprises a treatment strategy that uses photosensitizers to generate ROS like singlet oxygen, in order to eliminate cancer cells. In this context, Wei et al., developed a polyethylene glycol MPN loaded with the photosensitizer haemato porphyrin monomethyl ether (HMME) constituting the composite nanosystem $\text{MPN}@\text{HMME}$ for the treatment of tumors [152]. The $\text{MPN}@\text{HMME}$ exhibited selectively accumulation in cancer cells through the assistance of Folate and subsequent release of HMME. Moreover, when exposed to 638 nm near-infrared light irradiation, HMME was able to induce apoptosis in cancer cells without affecting normal cells. In addition, Dai et al., developed PEG-Ce6- $\text{Fe}^{\text{II}+}$ -gossypol MPNs by combining natural polyphenols, $\text{Fe}^{\text{II}+}$, and the photosensitizer Chlorin e6 (Ce6) to effectively carry out the antitumor impact of photodynamic therapy [153].

Photothermal therapy

Photothermal therapy (PTT) is a minimally invasive treatment technique that employs photothermal conversion agents (PTCAs) to gather at tumor locations and convert near-infrared light into heat energy [154]. When compared with other treatment methods, PTT offers the advantage of minimal harm to healthy tissues. This is due to its targeted action on areas with high concentrations of PTCAs and exposure to near-infrared light. Due to the significant assembly effect of polyphenols, MPNs have strong UV-vis absorbance in the near-infrared irradiation region. As a result, they serve as PTCAs in PTT treatments. In this context, Zhao et al., reported the successful fabrication of nanoscale Fe-EA MPN by utilizing EA, Fe, and polyvinylpyrrolidone for PTT of tumors [133]. The Fe-EA MPN demonstrated excellent biocompatibility and minimal cytotoxicity in both in vitro and in vivo experiments. In addition, it exhibited the ability to absorb near-infrared light and utilize its photothermal conversion capability to eliminate tumors without inducing significant toxic responses.

However, the clinical application of PTT are is plagued by the following challenge: the need to prevent excessive thermal damage to surrounding healthy tissues and mitigate the diminishing efficacy of PTT caused by the increased production of heat shock proteins [155]; Cao et al. employed quercetin and Fe ions to fabricate dynamically detachable MPN-based PTCAs ($\text{Qu-Fe}^{\text{II}+}\text{P}$), specifically targeting these concerns (Fig. 4A) [156]. The $\text{Qu-Fe}^{\text{II}+}\text{P}$ demonstrated commendable PTT effects when exposed to near-infrared light, while the presence of quercetin in $\text{Qu-Fe}^{\text{II}+}\text{P}$ aided in inhibiting the increase in heat shock proteins in vitro (Fig. 4B, C) and in vivo (Fig. 4D, E). These functions enabled the $\text{Qu-Fe}^{\text{II}+}\text{P}$ to accurately target and treat tumors at reduced temperatures (approximately 45 °C) (Fig. 4F, H). To summarize, MPN-based PTCAs, with their facile mode of synthesis, good biosafety, high photothermal conversion efficiency, and strong functional plasticity, comprise a significant research direction for PTT treatments.

TME modulation therapy

TME, or the tumor microenvironment, comprises a complex system consisting of diverse cells, lympho-vascular networks, and extracellular matrix, which is

(See figure on next page.)

Fig. 4 The PTT therapy application of MPN in cancer therapy. **A** The schematic representation of the PTT therapy of $\text{Qu-Fe}^{\text{II}+}\text{P}$. **B** The protein (**B**) and RNA (**C**) level expression of Heat shock protein 70(HSP70) with $\text{Qu-Fe}^{\text{II}+}\text{P}$ treatment in vitro **D**. The in vivo Hsp70 expression in tumors from mice 36 h with $\text{Qu-Fe}^{\text{II}+}\text{P}$ treatment as measured by immunofluorescence staining and Western blot (**E**). **F** The Photothermal imaging of mice after injection of $\text{Qu-Fe}^{\text{II}+}\text{P}$ under 808 nm irradiation. **G** Changes in tumor volumes and (**H**) digital photos of resected tumors after $\text{Qu-Fe}^{\text{II}+}\text{P}$ treatment. Reproduced with permission from Ref. [156]. Copyright 2019, ELSEVIER SCI LTD

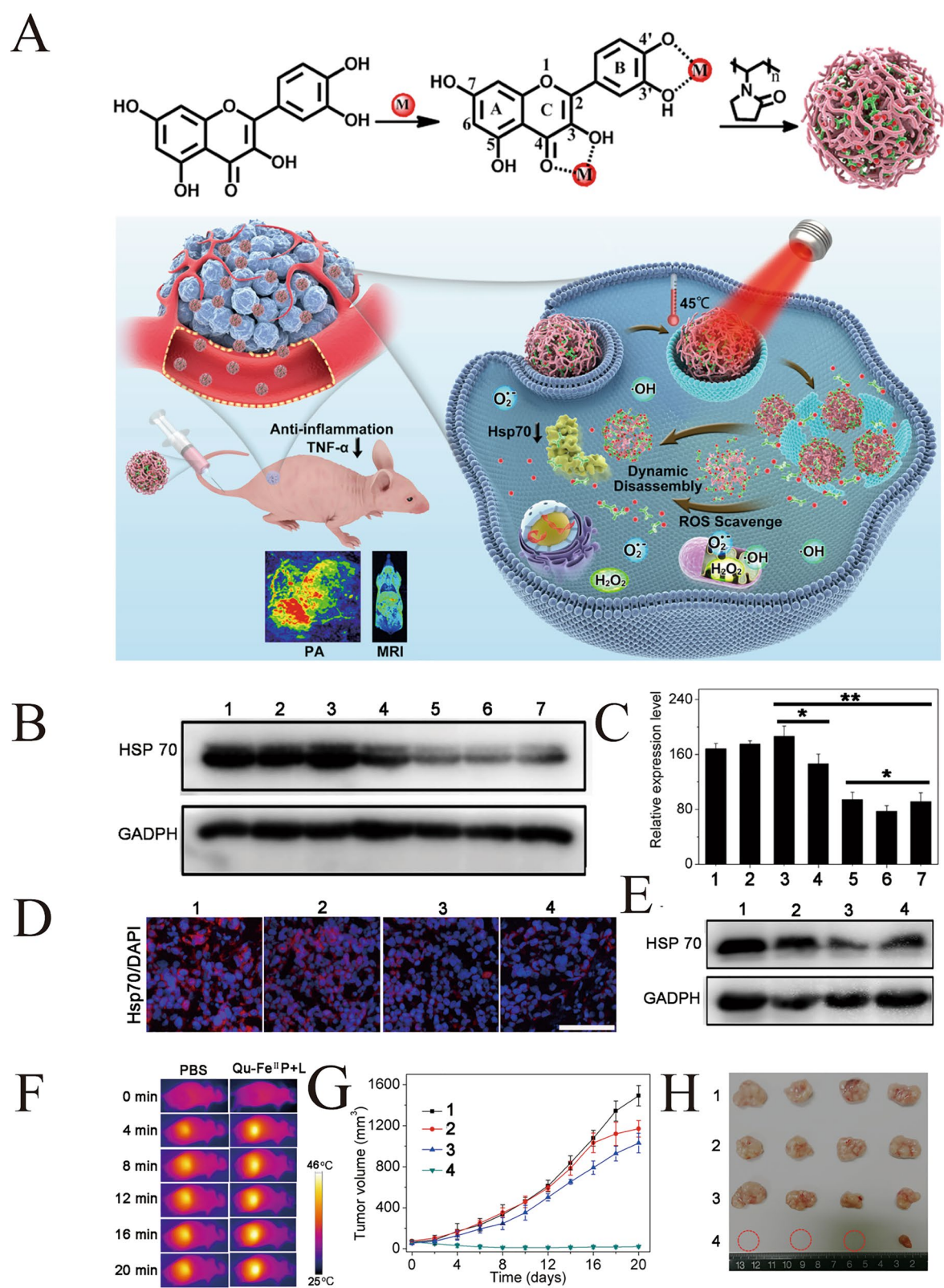


Fig. 4 (See legend on previous page.)

characterized by low pH values, hypoxia, among other factors. TME is an essential component of tumors and plays a significant role in their initiation and progression [157]. Thus, modulating the TME as a means of treating tumors (TME modulation therapy) shows great promise. However, TME modulation therapy is currently plagued by several challenges, including: (1) maintaining the circulation of nanoparticles; (2) infiltrating and enriching the tumor tissue; (3) penetrating the tumor cells; and (4) achieving controllable drug release [123]. Nonetheless, MPNs, by virtue of their inherent properties acquired through diverse assembly techniques and functionalization, can effectively overcome these challenges.

MPNs represent ideal nanoformulations for TME modulation, primarily due to two key factors: The intrinsic properties of polyphenols, including their anti-inflammatory, antioxidant, and antitumor characteristics; and the modular preparation strategy that facilitates the integration of functional molecules. Currently, MPN-based TME modulation therapies that are currently used, can be categorized into the following aspects: Antiangiogenesis, improvement of hypoxic conditions, regulation of endoplasmic reticulum stress (ERS), and reversal of immunosuppressive states. Angiogenesis plays a critical role in tumor growth and metastasis, with the TME serving as a fundamental basis for angiogenesis. The abundant vasculature within the TME supports tumor growth by delivering substantial amounts of oxygen and nutrients. Therefore, inhibiting angiogenesis presents a promising strategy for TME modulation. Specifically, the polyphenol structures within MPNs can suppress tumor angiogenesis through various mechanisms, including the inhibition of VEGF expression, restriction of epithelial-mesenchymal transition, reduction of matrix metalloproteinase expression, and inhibition of neovessels.

In terms of antiangiogenesis, Zhou et al., found that quercetin-based MPN nanoparticles (Q-NPs) could inhibit tumor growth by destroying existing blood vessels and suppressing the formation of new ones, thus exhibiting antiangiogenic properties (Fig. 5A) [158]. Upon intravenous administration, these Q-NPs were able to bind to upregulated VEGFR2 in the tumor vascular system, thereby inhibiting angiogenesis.

The hypoxic state of the TME promotes tumor growth while simultaneously reducing the efficacy of chemotherapy and oxygen-based therapies. Therefore, alleviating hypoxia is a crucial strategy for TME modulation. Currently, MPNs improve hypoxia in the TME through three primary mechanisms: (1) Oxygen delivery: The unique network structure of MPNs enables the loading and delivery of oxygen-releasing agents.

(2) In situ oxygen generation: MPNs can utilize agents such as MnO_2 to decompose H_2O_2 , thereby

producing oxygen and alleviating hypoxia in the TME. (3) Inhibition of oxygen metabolism: MPNs can generate H_2S gas, which suppresses mitochondrial oxygen consumption, effectively mitigating hypoxia. In terms of ameliorating the hypoxic TME, MPNs participate by facilitating the transport of oxygen, generating oxygen in situ, and regulating the metabolic oxygen pathways within tumor tissues. In this context, Sang et al., developed oxygen-enriched composite nanoparticles (Hb@Hf-Ce6 NPs) to improve the hypoxic state in TME, thereby enhancing the efficacy of tumor treatment (Fig. 5B) [159].

As a result of the atypical characteristics of TME (low pH, hypoxia, etc.), tumor cells frequently experience chronic endoplasmic reticulum stress. Thus, enhancing tumor cellular ERS comprises one of the strategies for TME modulation in therapy.

Currently, MPNs enhance tumor ERS through two primary approaches: 1) ROS-based therapy: This strategy induces oxidative stress in tumor cells, thereby increasing ERS and subsequently suppressing tumor growth; 2) Starvation therapy: This approach inhibits the supply of nutrients and energy, leading to enhanced ERS and the suppression of tumor progression. In this context, Wang et al., employed Fe-TA MPN to envelop a dendritic polymer containing an ERS-inducing drug (toyocamycin), resulting in the creation of a composite nanopatform (G5.NHAc-Toy@TF) for the treatment of tumors (Fig. 5C) [160]. The G5.NHAc-Toy@TF compound was able to generate cytotoxic hydroxyl radicals by undergoing Fenton reactions, thus amplifying ERS and leading to improved efficacy in vitro tumor treatment.

In addition, the TME frequently recruits a large number of immunosuppressive cells while diminishing the presence of cytotoxic T cells, resulting in the development of tumor immune tolerance [123]. The rich chemical bonds within the polyphenols of MPNs facilitate their efficient uptake by tumor cells and immune cells. Furthermore, MPNs can be engineered into immunogenic formulations, enhancing their functionality. As a result, MPNs hold significant potential for reversing the immunosuppressive state of the TME. Accordingly, Su et al., effectively developed a new and versatile nanoparticle vaccine by incorporating the antigen ovalbumin and the immunoreactive chlorogenic acid onto MPNs (Fig. 5D) [161]. The nanoparticle vaccine was able to stimulate cellular immune responses by activating the antigen presentation of dendritic cells while suppressing the activation of regulatory T cells. To summarize, MPN is an excellent nanopatform for TME modulation therapy because of its modular fabrication method and the integration of functional molecules.

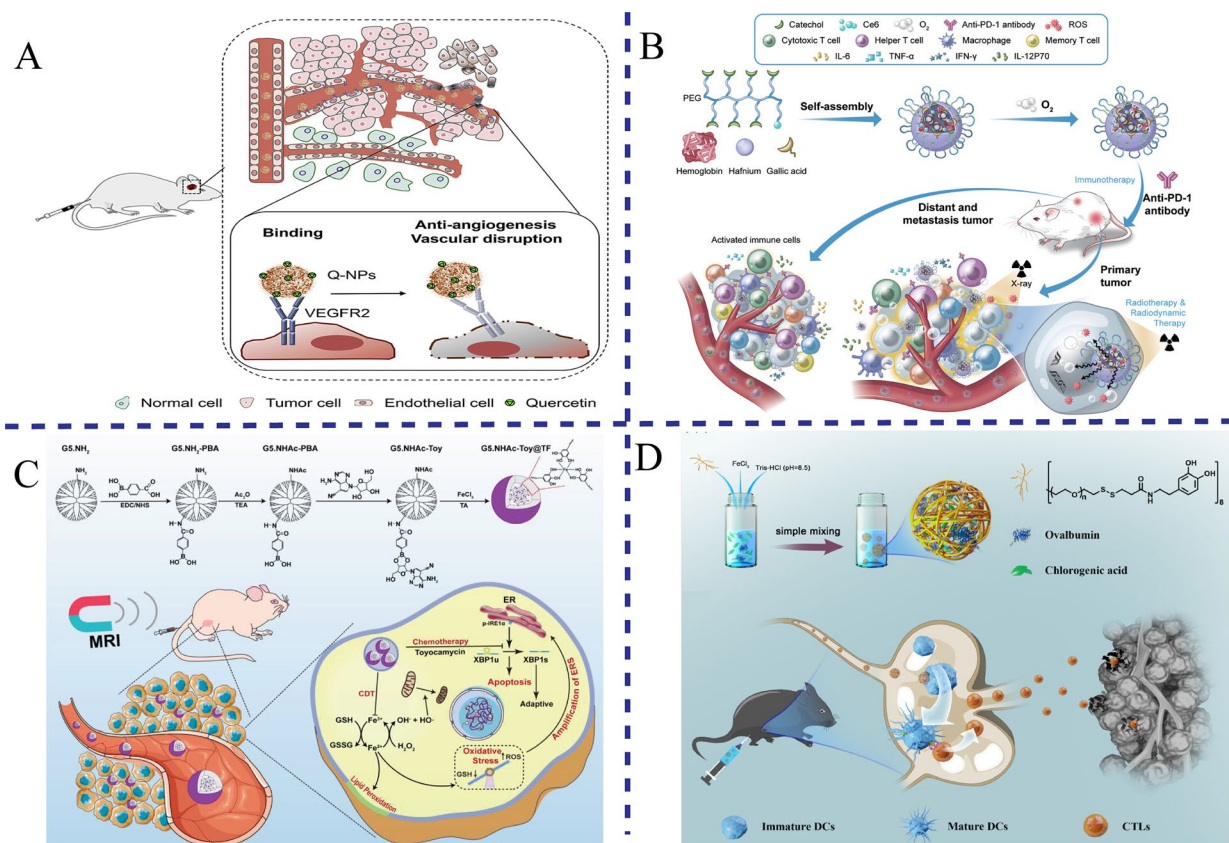


Fig. 5 The schematic illustration of TME immunomodulation therapy based on MPNs. **A** The schematic illustration of the anti-tumor effect of quercetin based MPN nanoparticles through anti-angiogenesis. Reproduced with permission from Ref. [158]. Copyright 2022, Elsevier. **B** The preparation and mechanism of oxygen-enriched composite nanoparticles (Hb@HF-Ce6 NPs) through relieve hypoxic state. Reproduced with permission from Ref. [159]. Copyright 2021, Wiley-VCH. **C** The schematic illustration of the anti-tumor mechanism of Fe-TA MPN to encapsulate composite nanoplateform (G5.NHAc-Toy@TF) through enhance ERS. Reproduced with permission from Ref. [160]. Copyright 2022, Wiley-VCH. **D** The schematic illustration of the preparation and process of MPNs@OVA + CHA for reversing immunosuppressive states. Reproduced with permission from Ref. [161]. Copyright 2023, Elsevier. ERS: Endoplasmic reticulum stress

Multimodal synergistic therapy

The combination of individual tumor therapies can result in a synergistic effect, leading to significant supra-additive effects where the outcome is greater than the sum of its parts (i.e., $1 + 1 > 2$) [162]. As MPNs are composites of metals and polyphenols, are particularly well-suited for integrating various therapy modes to achieve synergistic therapeutic effects [163, 164]. Accordingly, Fan et al., developed a nano system that integrated PTT and chemotherapy by applying a coating of Gd^{III+} -TA MPN onto gold nanorods that were loaded with a photothermal conversion agent [165]. The in vivo tests demonstrated that the nano system could reduce primary tumor volumes by 81% and arrest lung metastasis by 58%. Moreover, MPNs can also be utilized to enhance the combined effect of tumor photothermal therapy and photodynamic therapy. In this context, Zhang et al., developed a TME-responsive diagnostic and therapeutic nanoplateform (Ce6-GA@MnO₂-HA-PEG) that responded to the TME

and produced combined PDT and PTT effects, resulting in a synergistic effect [166]. When subjected to TME stimulation, the MnO₂ in the nanoplateform decomposed and released Mn^{II+} ions. These ions then combined with GA to create Mn^{II+}-GA MPN, which functioned as a photothermal converter. The generated oxygen also improved the efficacy of Ce6-mediated photodynamic therapy. Moreover, MPNs can integrate ferroptosis and apoptosis for tumor treatment. This is evident from the studies conducted by Hi et al., involving the combination of Fe^{III+}-TA MPN with bleomycin (BLM) and Prussian blue nanoparticles, which was loaded with a ferroptosis inducer (ML210) to create HMPB/ML210@TA-BLM-Fe^{III+} (HMTBF) nanocomposites [167]. The as-obtained nanocomposite was able to induce the process of tumor cell ferroptosis by releasing BML20 and facilitating the TA-mediated conversion of Fe^{III+} to Fe^{II+} through intracellular degradation. Additionally, the binding of Fe^{II+} with BLM can enhance the process of apoptosis in

tumor cells, thus synergizing with ferroptosis to effectively eliminate tumors.

These results all demonstrate that MPNs, as multifunctional nanoplatform, can combine various therapies to synergistically treat tumors. As observed, these findings clearly demonstrate that MPNs, acting as multifunctional nanoplatforms, can combine various therapies to effectively treat tumors through synergistic effects.

Antimicrobial application

Antimicrobial treatments have consistently relied on the inclusion of metal ions and metal compounds [29]. For instance, both silver ions and silver nanoparticles possess various mechanisms through which they exert their antimicrobial effects [168]. While metal ions possess exceptional antimicrobial properties, the excessive production of ROS during sterilization frequently damages adjacent healthy tissues [169]. Polyphenols possess inherent antioxidant properties, enabling MPNs to generate ROS for bactericidal purposes while concurrently mitigating oxidative stress-induced harm to healthy tissues [170, 171]. Thus, when compared to other antimicrobial agents, the benefits of MPNs in antimicrobial applications include:

(1) MPNs exhibit excellent stability and responsiveness to changes in pH; (2) MPNs possess the ability to gradually release metal ions, thereby extending their effectiveness; (3) The presence of polyphenols in MPNs can mitigate the potential toxicity associated with metal ions. (4) MPNs exhibit substantial photothermal conversion properties [30, 172]. Based on these advantages, the application of MPNs in antimicrobial research primarily employs the following approaches: (1) MPNs encapsulate photosensitizers to generate ROS for bactericidal purposes; (2) MPNs exploit their ability to respond to stimuli in order to selectively release antimicrobial drugs; (3) MPNs discharge metal ions as a means to eliminate bacteria; 4) MPNs encapsulate photothermal inducer for the purpose of sterilization.

In the context of MPN-mediated ROS antimicrobial research, Wang et al., developed stimulus-responsive nanoparticles by encapsulating chitosan and Ce6 with Mg-EGCG MPN, thereby resulting in antibacterial effects (Fig. 6A) [173]. The in vitro experiments demonstrated that the composite nanoparticles effectively eliminated bacteria within a span of 10 min when exposed to near-infrared light (Fig. 6B). In addition, the in vivo

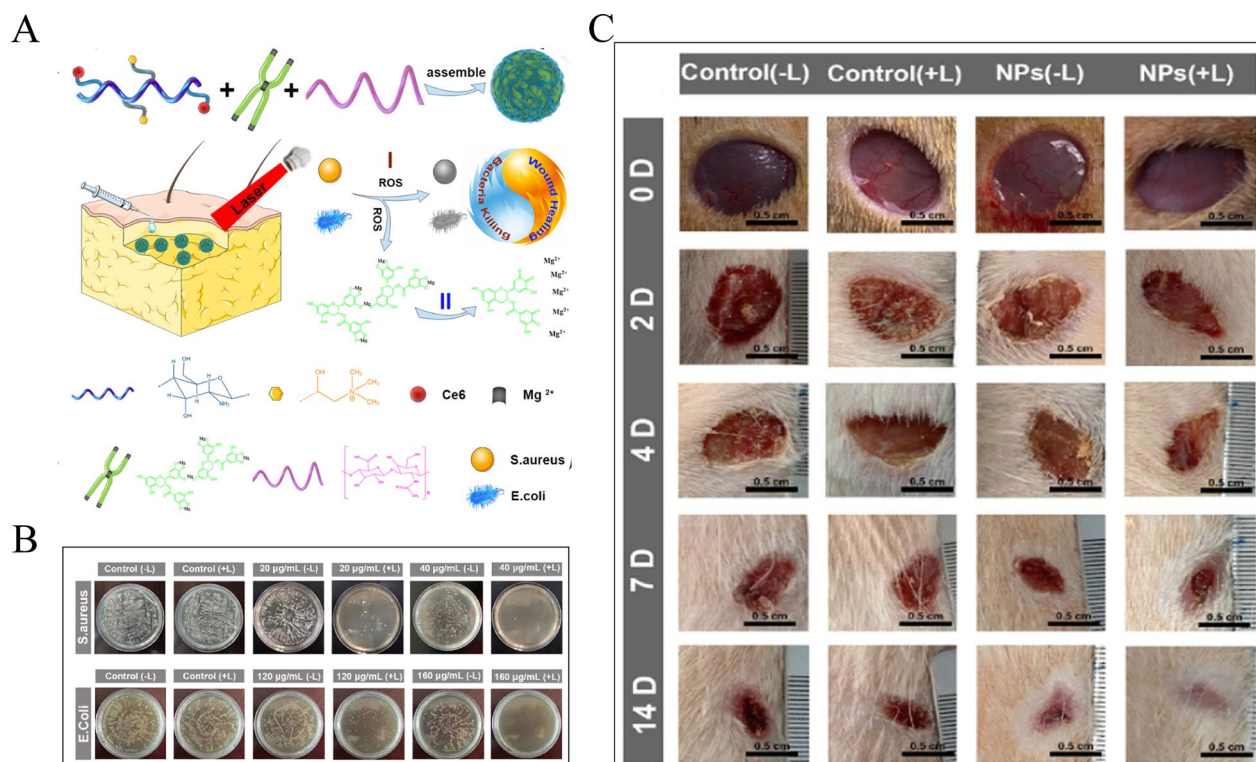


Fig. 6 The anti-bacteria application of MPNs. **A** The schematic representation of the antibacterial Mechanisms of HTCC-Ce6 and Mg/EGCG Complex. **B** Colony-forming experiment of *E. coli* and *S. aureus* Following Treatment with NPs with or without light irradiation (660 nm, 100 mW cm⁻², 10 min). **C** The photographs of wound closure on 0, 2, 4, 7, and 14 days in *S. aureus*-infected SD rat models. Reproduced with permission from Ref. [173]. Copyright 2019, ACS

experiments showed that the hydrogel effectively controlled wound infections and successfully promoted wound healing (Fig. 6C). These composite nanoparticles had the ability to generate ROS when exposed to near-infrared light, which could be used for sterilization. Additionally, the Mg-EGCG MPN nanoparticles would release Mg in response to ROS, which promoted wound healing. Among the metal ions with antimicrobial action, rare earth metal ions ($\text{Re}^{\text{III}+}$) have notable antimicrobial properties as they are capable of substituting the binding sites for $\text{Ca}^{\text{II}+}$ on bacterial membranes, thereby exerting a significant antibacterial effect [79]. Liu et al., fabricated a composite antibacterial nanocoating by combining catechin and rare earth metal ions ($\text{Re}^{\text{III}+}$) [174]. The findings demonstrated that the antibacterial nanocoating exhibited robust antibacterial and anti-adhesion properties against *Pseudomonas aeruginosa*, effectively inhibiting the formation of biofilms. Furthermore, in the context of MPN-mediated PTT antimicrobial research, Deng et al., utilized $\text{Fe}^{\text{III}+}$ -TA MPN nanoparticles in an agarose-based composite hydrogel to investigate the antimicrobial properties of PTT in treating wound infections [175].

Anti-inflammatory application:

Key processes in the treatment of inflammatory diseases involve reducing levels of ROS, inflammatory cytokines, and promoting the transition of macrophages from the M1 to the M2 type. MPNs often exhibit strong redox activity and anti-inflammatory properties due to their geometric similarity to active metal sites found in various antioxidant enzymes [176]. For instance, Qin et al., successfully synthesized $\text{Cu}^{\text{II}+}$ -EGCG MPN, a compound consisting of the antioxidant EGCG and the anti-inflammatory metal ion $\text{Cu}^{\text{II}+}$, and effectively utilized it for the treatment of osteoarthritis (OA) [177]. The resulting $\text{Cu}^{\text{II}+}$ -EGCG MPN demonstrated the ability to effectively eliminate intracellular ROS, resulting in a significant reduction of pro-inflammatory cytokine levels in vitro. Moreover, in the context of treating OA, Guo et al., conducted a study on the ability of $\text{Sr}^{\text{II}+}$ -TA MPN coating to scavenge ROS and inflammatory factors, while also investigating its protective effects on cartilage [178]. Besides exhibiting anti-inflammatory and antioxidant properties, the MPN coating also demonstrated a retardation in the advancement of OA in a rat model. In addition, Yang et al. fabricated $\text{Cu}^{\text{II}+}$ -EGCG MPN capsules with significant anti-inflammatory properties aimed at treating peripheral artery disease (PAD) by reducing cellular ROS levels and inflammatory cytokines, while promoting vascular regeneration [179, 180]. There in vitro and animal studies showed that these MPN capsules increased VEGF expression and stimulated vascular repair, addressing PAD's inflammatory nature and aiding effective therapy.

Bone regeneration

The utilization of MPNs in bone tissue regeneration primarily encompasses two strategies: (1) directly stimulating osteogenic differentiation and (2) inducing osteogenesis via immunomodulation. Osteogenic metal ion based MPNs primarily enhance the process of osteogenic differentiation in the field of bone tissue engineering. AnJani et al., reported that the combination of Kaempferol, a flavonoid compound, with $\text{Zinc}^{\text{II}+}$ resulted in the formation of $\text{Zinc}^{\text{II}+}$ -Kaempferol MPN composites with excellent in vitro and in vivo osteogenic functions [181]. Even at concentrations as high as 25 μM , $\text{Zinc}^{\text{II}+}$ -Kaempferol MPN demonstrated excellent biocompatibility and significantly increased osteoblast activity in vitro. Furthermore, the in vivo experiments conducted on live zebrafish showed that $\text{Zinc}^{\text{II}+}$ -Kaempferol MPN stimulated the process of osteogenic differentiation in adult fish. In addition, Lee et al., coated Ti surfaces with $\text{Mg}^{\text{II}+}$ -EGCG MPN to enhance the bone integration process (Fig. 7A) [182]. In vitro, the $\text{Mg}^{\text{II}+}$ -EGCG MPN-coated Ti was found to significantly promote mineralization levels and mRNA expression of osteogenic genes in human adipose-derived mesenchymal stem cells (Fig. 7B–D), while concomitantly reducing osteoclastogenic differentiation in RAW264.7 cells (Fig. 7E, F). The primary principle for promoting bone tissue regeneration through immunomodulation is the regulation of macrophage polarization. Accordingly, Zhang et al., utilized $\text{Cu}^{\text{II}+}$ -TA MPN to coat porous polymer scaffolds for the purpose of regenerating bone defects in periodontal tissue [183]. The experimental results demonstrated that the $\text{Cu}^{\text{II}+}$ -TA MPN coating effectively inhibited the inflammatory response of macrophages and promoted angiogenesis, thereby leading to the promotion of bone regeneration.

Medical imaging

Medical imaging technology is essential for diagnosing diseases, creating treatment strategies, and assessing the effectiveness of therapies [184, 185]. With the development of nanomaterials, medical imaging technology has also seen significant advancements. Current nanoscale medical imaging agents include quantum dots, magnetic nanoparticles, among others. Although these nanoscale agents offer many advantages over traditional contrast agents, they still cannot fully meet the increasingly high requirements of modern medical imaging technology. Due to the properties of metal ions and the porous network of MPNs, MPNs have become an important type of contrast agent in medical imaging [186]. The primary applications of MPNs in medical imaging encompass

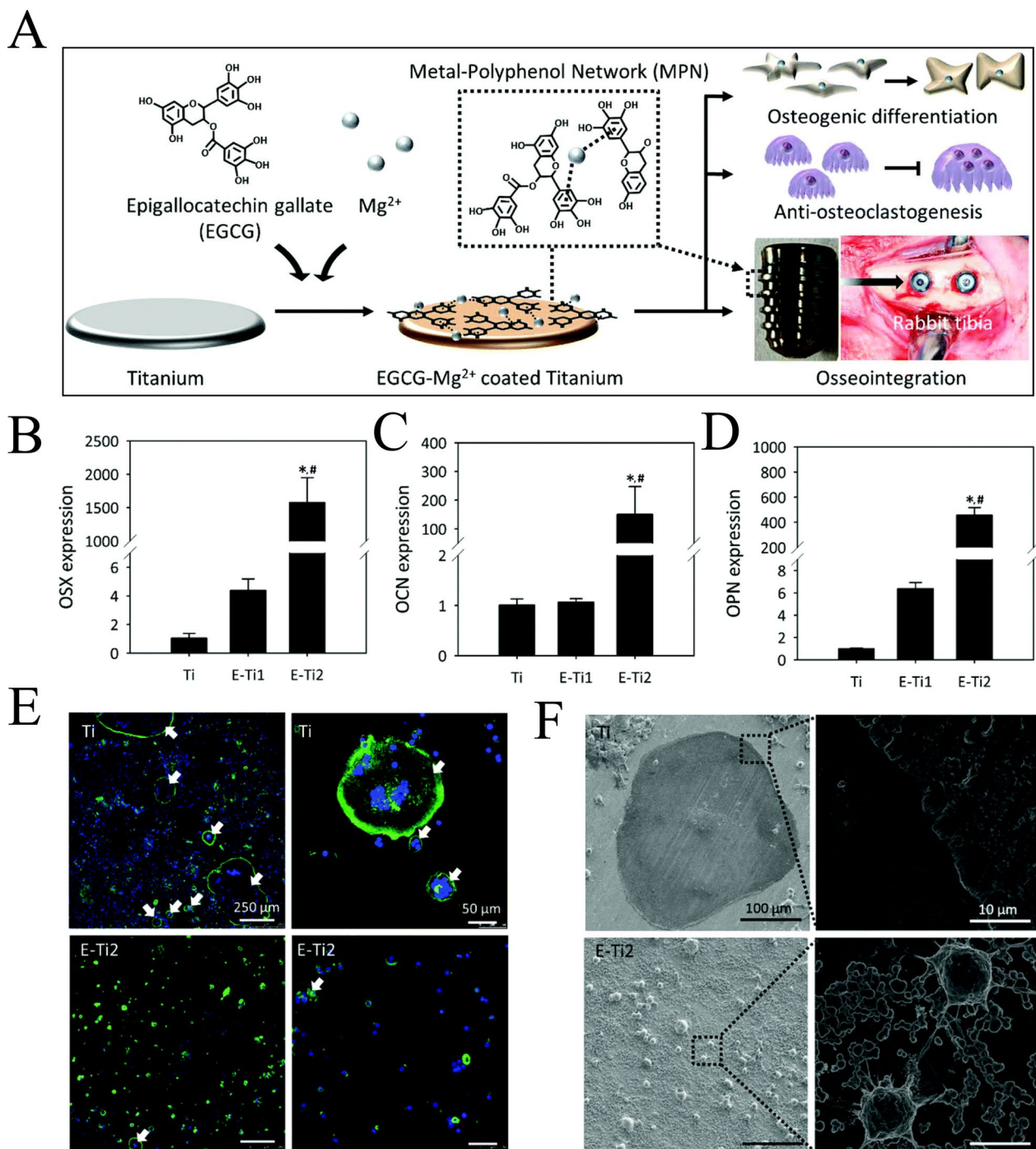


Fig. 7 The promoting bone formation of MPNs. **A**. The schematic representation of the epigallocatechin gallate-magnesium (EGCG- Mg^{II}) MPN coating applied to a titanium alloy surface for orthopedic applications. The osteogenic gene: **(B)** OSX, **(C)** OCN, **(D)** OPN expression of hADSCs after cultured on EGCG- Mg^{II} coated Ti in vitro. **E** The Confocal images shows the RAW264.7 cultured on EGCG- Mg^{II} coated Ti can inhibited the osteoclastic differentiation; **(F)** The SEM images shows the RAW264.7 cultured on EGCG- Mg^{II} coated Ti can inhibit the osteoclastic differentiation. Reproduced with permission from Ref. [182]. Copyright 2020, RSC

both single-mode imaging and multimodal imaging. Single-mode imaging encompasses various techniques such as MRI, CT, PET, US, FLI, PAI, and others.

MRI, a widely used imaging technique in medicine, primarily differentiates between normal and abnormal tissues by administering contrast agents intravenously

[187]. Zhang et al., developed a biocompatible metal-polyphenol nanoparticle specifically for the detection and treatment of Glioblastoma multiforme [188]. These RPDGs had the ability to induce to trigger apoptosis and ferroptosis in tumor cells, while also display excellent MRI imaging capabilities. Moreover, MPNs also possess the ability to perform PET imaging due to the radiolabel properties of metal ions. For instance, Guo et al., employed TA and various metals to fabricate MPN capsules for MRI and PET imaging (Fig. 8A, B) [101]. The $\text{Cu}^{\text{II}+}$ -TA MPN, in particular, demonstrated high efficacy for PET imaging. In the field of ultrasound imaging, Caruso et al., utilized CaCO_3 as a template to construct $\text{Fe}^{\text{III}+}$ -TA MPN nanoparticles [189]. Because MPN nanoparticles possess the ability to catalyze the conversion of H_2O_2 into O_2 microbubbles, these $\text{Fe}^{\text{III}+}$ -TA MPN nanoparticles could be successfully used in ultrasound imaging to diagnose internal levels of H_2O_2 (Fig. 8C). Fluorescent imaging technology is extensively utilized in optical imaging, primarily for the real-time, dynamic, and non-invasive detection of tumors. In the context of MPNs in fluorescent imaging, Pan et al., encapsulated the PF-127 near-infrared dye within MPNs to enable the visualization of tumors using near-infrared fluorescent imaging and PET imaging (Fig. 9A) [190]. The in vivo experiments

demonstrated that the tumor tissue exhibited a significantly higher fluorescence intensity compared to the normal tissue when exposed to the PF-127 encapsulated MPN (Fig. 9B, C).

In comparison to single-mode imaging, multimodal imaging technology combines multiple imaging systems to achieve synergistic effects [191]. In this context, Chen et al., employed $\text{Fe}^{\text{III}+}$ or $\text{Mn}^{\text{II}+}$ as crosslinking agents to encapsulate DOX and simvastatin within polyphenolic polymers for the purpose of dual-imaging-guided tumor therapy using PET/MRI [192]. The resulting nanoplatform demonstrated prolonged circulation in the bloodstream and significant accumulation in tumor tissue, as evidenced by MRI and PET tests. The excellent near-infrared light absorption capability of MPNs not only endows them with the ability for efficient photothermal conversion but also enables their use for superior optical imaging (PAI). In this context, Cai et al., prepared composite nanoparticles ($\text{Fe}^{\text{III}+}$ -PDA-ICG NPs) by loading indo-cyanine green (ICG) onto $\text{Fe}^{\text{III}+}$ -PDA MPN for integrated tumor diagnosis and therapy under the guidance of PAI/MRI dual-imaging (Fig. 8D) [193]. As observed, due to their versatility and ability to perform multiple functions, the use of MPNs as multifunctional nanoplatforms in medical imaging is extensive and prevalent.

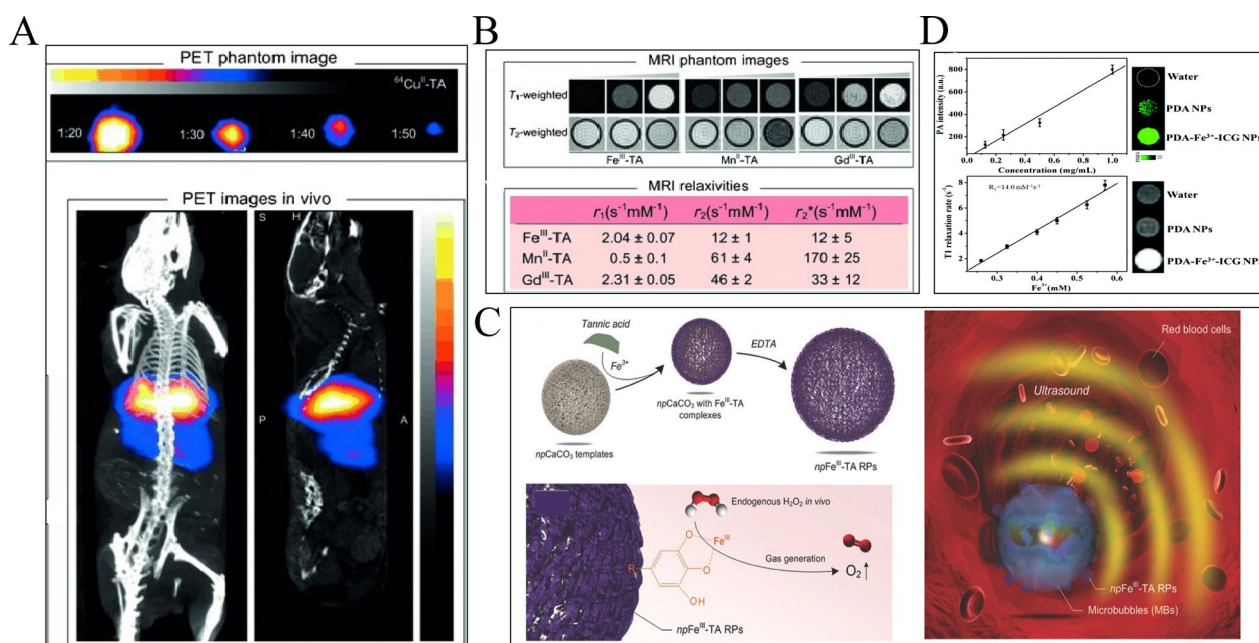


Fig. 8 The PET, MRI, and PA imaging application of MPNs. **A** The PET image of an in vivo model after injection of $\text{Cu}^{\text{II}+}$ -TA MPN capsule. **B** The MRI phantom image and MRI relaxivities of MPN capsules. **A, B** reproduced with permission from Ref. [101]. Copyright 2014, Wiley-VCH. **C** Schematic illustration for the preparation of $\text{npFe}^{\text{III}+}$ -TA RPs to probe H_2O_2 in vivo by ultrasound (US) imaging. Reproduced with permission from Ref. [191]. Copyright 2015, Wiley-VCH. **D** The PA and MRI prosperity of $\text{PDA-Fe}^{\text{III}+}$ -ICG NPs in vitro. Reproduced with permission from Ref. [195]. Copyright 2016, RSC

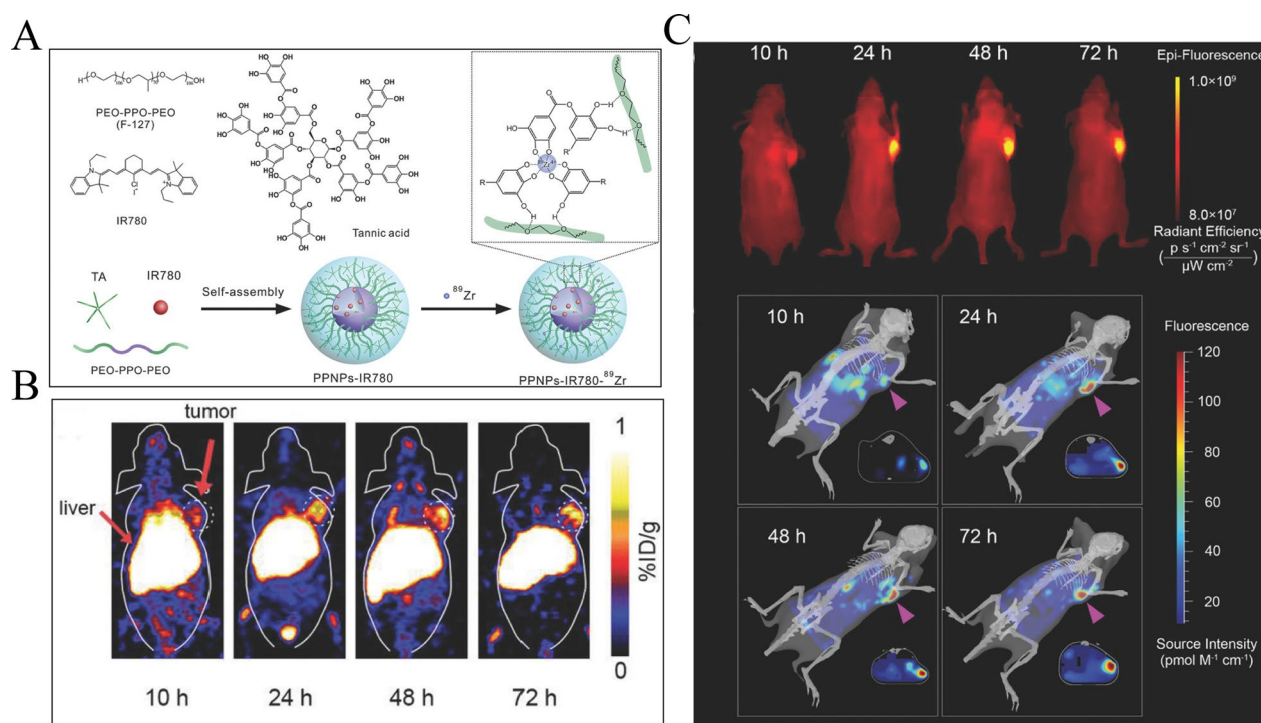


Fig. 9 The PET and fluorescence images application of MPNs. **A** the schematic presentation of preparation of PPNPs-IR780-89Zr. **B** The PET images at 10, 24, 48, and 72 h post intravenous injection of PPNPs-IR780-89Zr. **C** The NIR fluorescence images and 3D fluorescence images of mouse at 10, 24, 48, and 72 h post intravenous injection of PPNPs. Reproduced with permission from Ref. [192]. Copyright 2018, Wiley-VCH

Others

In addition to the aforementioned applications, MPNs are also utilized in the management of Alzheimer's disease, cell encapsulation, and protection, among other purposes. The amyloid hypothesis suggests that the accumulation of amyloid β -peptide ($A\beta$) in brain tissue plaques may be responsible for the development of Alzheimer's disease [194]. Hence, inhibiting the accumulation amyloid proteins $A\beta$ could serve as a promising therapeutic approach for treating Alzheimer's disease [195]. Due to the specific chelation sites between the histidine parts of $A\beta$ and transition metals such as Ni^{II+} and Co^{II+} , certain MPNs can effectively inhibit $A\beta$ [196]. In this context, Caruso et al., conducted a study to examine how different MPN coatings affect gold nanoparticles in their ability to prevent the formation of amyloid protein $A\beta$ [197]. Their findings indicated that all nanoparticles were able to inhibit the formation of amyloid protein $A\beta$. In particular, nanoparticles coated with Cobalt $^{III+}$ -TA MPN exhibit the most significant inhibitory effect, with a rate of 90%. Moreover, the molecular dynamics simulations also indicated that the superior inhibitory activity of Cobalt $^{III+}$ -TA MPN could be attributed to the specific geometric configuration of the cobalt coordination sites, which enabled effective interaction with the histidine in

amyloid protein $A\beta$. Thus, MPNs are regarded as a promising therapeutic approach for Alzheimer's disease.

MPNs serve as an effective biointerface coating material, capable of encapsulating bacteria or cells to provide protection. For instance, Li et al., developed a Fe^{III+} -TA MPN coating on the surface of cells as a means of safeguarding them against harm from external factors like ultraviolet radiation and reactive oxygen species [198]. The Fe^{III+} -TA MPN coating exhibited superior properties compared to conventional coatings. Furthermore, it could be disassembled in real-time when exposed to external stimuli and demonstrates excellent biocompatibility and biosafety. Thus, the technique of cell encapsulation using MPN coatings can be employed for a wide range of living cells, facilitating scientific investigation and potential utilization of live cells in diverse domains.

The biosafety and fate of MPN in vivo

In vitro biosafety

The increasing utilization of MPNs in nanomedicine has raised significant concerns regarding their biocompatibility and safety within a biological setting. Although metal ions are crucial for life, they still carry the potential for long-term toxicity [199]. Fortunately, the potential toxicity of metal ions can be mitigated by

chelating them with polyphenolic substances [77]. The biocompatibility of MPNs can be evaluated through both in vitro and in vivo assessments. Accordingly, multiple studies have verified that MPNs demonstrate favorable biocompatibility and minimal cytotoxicity in vitro. Using the widely employed MPN types ($\text{Fe}^{\text{III+}}/\text{Fe}^{\text{II+}}$ -TA networks) as a case study, Ko et al., performed experiments in which fibroblasts were cultured with $\text{Fe}^{\text{III+}}$ -TA MPN coatings and $\text{Fe}^{\text{II+}}$ -TA MPN coatings for a duration of 24 h to assess their cell viability [200]. The MTT assay results demonstrated that the cell viability in the groups cultured with different MPN coatings was greater than 80% (Fig. 10A). This suggests that networks composed of $\text{Fe}^{\text{III+}}/\text{Fe}^{\text{II+}}$ -TA exhibit favorable biocompatibility and hold promise as potential candidates for nanomedical applications.

In addition to evaluating cell viability, alterations in cell morphology serve as an indicator of MPN's in vitro biological safety. Li et al., utilized scanning electron microscopy (SEM) to analyze the morphological alterations of MC3TC-E1 cells following a three-day co-culture with Mg-phenolic MPNs at different concentrations [201]. The SEM micrographs revealed that, following a three-day period of co-culture, cells treated with Mg-phenolic MPNs exhibited noticeable signs of increased cell growth and higher biocompatibility with the surrounding environment, as compared to the control group (Fig. 10B). As observed, numerous studies have shown that MPNs exhibit favorable biosafety characteristics in vitro.

Biosafety and immunotoxicity in vivo

The biocompatibility of nanomaterials is an essential requirement for their successful application in clinical settings. Zhou et al., investigated the biosafety of the $\text{Mn}^{\text{II+}}$ -TA MPN nano system in a mouse model [202]. The experimental data indicated that the mice's body weight, histopathological examination using HE staining of major organs (such as heart, liver, lungs, etc.), and biochemical indicators in the blood all fell within the normal range (Fig. 10C). Furthermore, the biodegradability of the $\text{Mn}^{\text{II+}}$ -TA nano system was assessed through the utilization of inductively coupled plasma optical emission spectrometry. The results revealed that around 80% of $\text{Mn}^{\text{II+}}$ was eliminated from the body within a span of 96 h. The results indicate that MPNs exhibit favorable in vivo biosafety. Given that the body's immune cells typically identify metal ions and their complexes as foreign antigens [203], it is important to consider the potential immunotoxicity of MPNs in vivo. The induction of immunotoxicity by metal ions and their complexes involves a complex interplay of mechanisms, including oxidative stress, inflammatory responses, autophagy and apoptosis, organelle damage and functional disorders, genetic material changes, immunosuppression, and disruption of metal homeostasis [203]. However, the immunotoxicity of MPNs may be reduced in comparison to that of individual metal ions due to the chelating properties of polyphenolic substances.

Steven et al., performed an experiment to evaluate the in vivo biosafety and immunogenicity of MPNs by subcutaneously injecting an MPN gel into mice [204]. Following

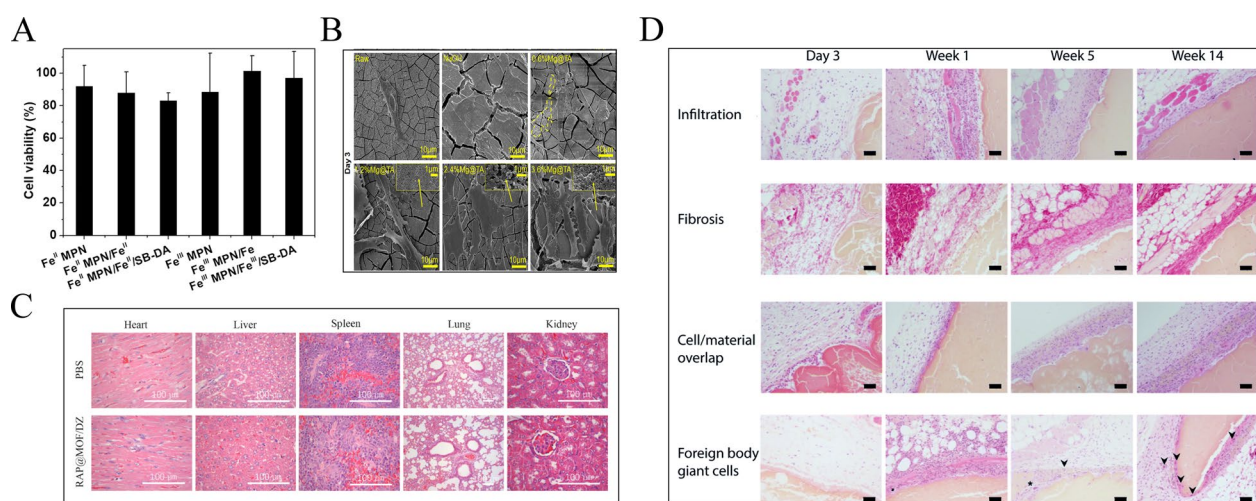


Fig. 10 The biosafety and immune of MPN in vitro and in vivo. **A** The Cytotoxicity of different MPN group to NIH-3T3 fibroblasts. Reproduced with permission from Ref.[200]. Copyright 2020, Elsevier. **B** The effect of the $\text{Mg}^{\text{II+}}$ -TA MPN on cell morphology after 3 days of co-culture with cells in vitro. Reproduced with permission from Ref. [201]. Copyright 2019, ACS. **C** The histology images of H&E staining slices for the major organs (heart, liver, spleen, lung, and kidney) obtained from mice treated with PBS or RAP@MOF/DZ. Reproduced with permission from Ref. [202]. Copyright 2020, ACS. **D** The low immunotoxicity of Ti-Ta gel in vivo after subcutaneous injection. Reproduced with permission from Ref. [204]. Copyright 2019, RSC

the subcutaneous injection of the Ti-Tannic gel, a mild inflammatory response was triggered, and the gel underwent gradual degradation (Fig. 10D). Additionally, no difference in the titanium concentration was observed in the brain, heart, kidneys, and lung tissues of the treated mice, when compared to the control group that did not receive the Ti-Tannic gel injection. These studies suggest that MPNs have favorable biosafety and minimal immunotoxicity in the *in vivo* microenvironment.

The fate of MPN in vivo

The trajectory of nanocomposite materials within the human body, until their final outcome, can generally be divided into four distinct processes: Administration, Bio-distribution, Metabolism, and Elimination, collectively referred to as ADME (Fig. 11) [205]. The following section examines each of these four aspects separately to elucidate the absorption, distribution, and the eventual fate of the MPN nanoplateforms *in vivo*.

Administration

In order to exploit the therapeutic benefits, nanomaterials must initially penetrate the body through different methods of administration. At present, the use of nanocomposite materials is mainly done through

methods like injection (intravenous, subcutaneous, intratumoral, etc.), inhalation, dermal administration, and others (Fig. 11A) [206]. Each exposure method possesses its respective advantages and disadvantages; for instance, although intravenous injection can rapidly deliver nanomaterials throughout the body, it also renders them more susceptible to clearance by the body's kidneys and liver. In contrast, subcutaneous and intratumoral injections can overcome the shortcomings of systemic medication by acting directly on the affected area. Inhalation is another mode of drug delivery, mainly used in pulmonary diseases and systemic delivery of medications. For inhaled nanomedicine, the smaller the size, the more likely it is to deposit within the lung parenchyma [207]. Oral administration is commonly favored for nanomedicines due to its non-invasive nature. However, enzymatic degradation, gastric acids, and intestinal barriers have a substantial effect on the bioavailability of nanomedicines [208]. Dermal administration is commonly used for lipophilic nanomedicines with a molecular weight less than 600 Da. As MPNs are mostly in the form of nanoparticles, nano capsules, and so on, injection remains the most frequently utilized method of administration for MPN [209–211].

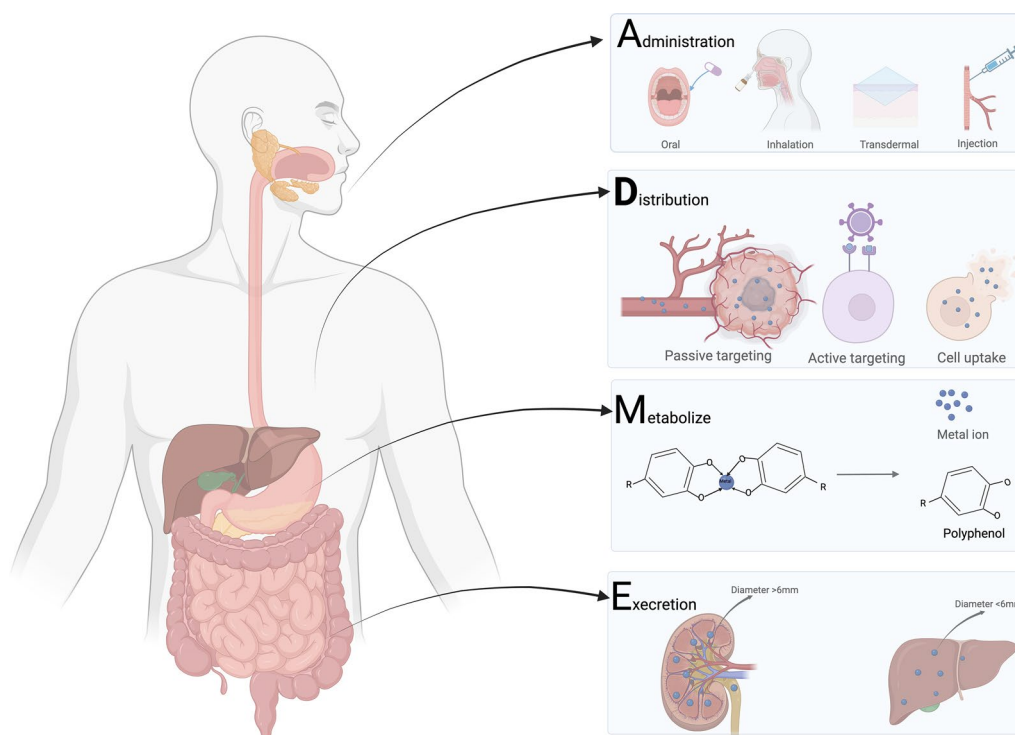


Fig. 11 The fate journey of MPN in human body: ADME. The process can be divided into four parts: administration; distribution; Metabolism and Excretion. This figure was drawn by biorender.com

Biodistribution

The biodistribution of composite nano systems upon entering the body is a critical process that directly impacts their therapeutic efficacy. The distribution patterns of nanocomposite systems in the body can be categorized into three types: passive targeting, cellular uptake, and active targeting (Fig. 11B) [205].

The main mechanism of passive targeting relies on the phenomenon in which particular macromolecules have a higher tendency to permeate and accumulate in tumor tissues. This process is known as the enhanced permeability and retention (EPR) effect [212]. Multiple studies have shown that nanocarrier systems based on MPNs exhibit notable passive targeting abilities, particularly by accumulating in tumor tissues [134, 156]. In this context, Mao et al. utilized EGCG, phenolic platinum (IV) pro-drug (Pt-OH), and polyphenol modified block copolymer (PEG-b-PPOH) as the building blocks to create complex nanomedicine (PTCG NPs), which possess the ability to eliminate tumor [213]. The ideal range for EPR (10–200 nm) was achieved by adjusting the diameter of the PTCG NPs. Consequently, animals in the PTCG NPs injected group had eight times more intratumoral platinum than those in the cisplatin alone group due to the EPR impact of PTCG NPs. When PTCG NPs were used in clinical settings, their EPR action greatly increased circulation time and tumor accumulation in comparison to cisplatin, strengthening the anti-tumor efficacy and lowering systemic toxicity.

Cells internalize nanomaterials through two separate endocytic pathways: pinocytosis and phagocytosis [214, 215]. Pinocytosis is a process that usually involves the uptake of fluids and tiny molecules through small vesicles that have a diameter of less than 0.15 μm . On the other hand, phagocytosis involves the internalization of larger particles through phagosomes that have a diameter greater than 0.25 μm . Zhou et al., examined the process of internalization of $\text{Mn}^{\text{II}+}$ -TA MPN-based nano systems [202]. The confocal fluorescence microscopy studies demonstrated strong cytoplasmic fluorescence signals originating from the $\text{Mn}^{\text{II}+}$ -TA MPN group, indicating efficient cellular internalization.

Due to its high level of specificity, active targeting is frequently considered the optimal method for distributing composite nanocomponents within the body. In this context, Caruso et al., utilized the precise recognition between antigens and antibodies to create nanoparticles coated with MPN, which possess the ability to actively target specific sites [216]. The design involved using a group of nanoparticles coated with MPNs, specifically $\text{Fe}^{\text{III}+}$, $\text{Cu}^{\text{II}+}$, $\text{Co}^{\text{II}+}$, and $\text{Ni}^{\text{II}+}$. All of these nanoparticles showed potential for active targeting. However, the $\text{Co}^{\text{II}+}$ -TA MPN exhibited a specific binding increase of

more than two times compared to the others. Additionally, Ju et al., synthesized MPN capsules by employing CaCO_3 as a template, enabling drug encapsulation and selective targeting of cancer cells [104]. At first, employing a phenol-functionalized hyaluronic acid and polyethylene glycol coating, the study created cross-linked MPN capsules that selectively bind to CD44^+ cells. These capsules, when loaded with anti-cancer drugs, demonstrated increased toxicity toward targeted CD44^+ cells, while reducing non-specific toxicity.

To summarize, the biodistribution of MPNs within the body is frequently encountered as a crucial factor that impacts their therapeutic efficacy. Correspondingly, an optimal distribution of MPNs should prioritize their concentration in the affected tissue regions while minimizing their presence in healthy tissues, thereby minimizing the toxic effects on normal organs.

Metabolism and excretion

Prior to elimination from the body, nanomedicines must undergo the metabolic processes of the body. Non-biodegradable nanomedicines are excreted without being broken down, whereas biodegradable nanomedicines are broken down before excretion (Fig. 11C) [217]. Due to their sensitivity to external stimuli, MPNs have a tendency to degrade during metabolism and subsequently be eliminated from the body [105].

As observed, the ultimate fate of nanomaterials in the body is either accumulation or excretion (Fig. 11D). Nanoparticles that do not accumulate in organs and tissues are excreted by the body. Increased nanoparticle circulation duration and reduced clearance rate enhance the probability of their accumulation through interactions with tissues and organs. The body eliminates nanoparticles through different pathways, such as renal clearance, hepatic clearance, mucociliary clearance, gastrointestinal tract clearance, and clearance by the reticuloendothelial system (RES) [206]. Given the biodegradable characteristics of MPNs, the concentration of metallic ions can be measured to determine the levels of MPN-based nano systems [218]. Renal clearance is the fastest and safest way to eliminate substances from the body; however, it is limited to nanoparticles that have a diameter of less than 6 nm [219–221]. The hydrodynamic diameter of composite nanocomponents is a key factor in determining renal clearance. In order to assess the impact of hydrodynamic diameter on MPNs on their removal from the body, Liu et al., developed pH-sensitive nanodots (Fe -CPND) for the treatment of tumors by utilizing $\text{Fe}^{\text{III}+}$, EGCG, and poly(vinylpyrrolidone) [222]. The Fe -CPND nanoparticles had a hydrodynamic diameter of approximately 5.4 nm and exhibited a neutral surface charge. Additionally, animal models subjected to MRI scans exhibited

prompt signal enhancement in the kidneys and bladder subsequent to the intravenous administration of Fe-CPND nanoparticles. The signal intensity in the kidneys and bladder commenced diminishing 1.5 h post-injection and subsequently returned to baseline levels after 24 h. Correspondingly, the urinalysis conducted during the treatment revealed a progressive increase in the concentration of Fe ions and the MRI signal. These findings indicate that Fe-CPND nanoparticles can be efficiently eliminated via renal excretion.

Hepatic clearance becomes the primary method of excretion for nanoparticles that are not able to be eliminated by the kidneys. Nanoparticles are eliminated by the liver via the following specialized epithelial cells: (1) hepatocytes; (2) phagocytic Kupffer cells. Hepatocytes and Kupffer cells have distinct functions in clearing different types of nanoparticles. Hepatocytes are responsible for clearing cationic nanoparticles, while Kupffer cells primarily clear anionic nanoparticles [223–226]. Hepatocytes uptake nanoparticles via endocytosis and enzymatic activity, and subsequently eliminate them into the small intestine through bile, resulting in their excretion with feces [227]. On the other hand, Kupffer cells phagocytose nanoparticles and retain the captured material within the RES for clearance [228]. The RES is comprised of a network of macrophages distributed throughout different organs [229], primarily responsible for removing substances from the blood and lymph nodes. RES cells are distributed throughout various organs, with a higher

concentration in the liver. Due to the slow clearance of nanoparticles by the mononuclear phagocyte system (MPS) in the RES, there is an increased risk of toxicity to the organism. In general, Kupffer cells exhibit greater efficacy in the removal of nanoparticles compared to hepatocytes.

Renal clearance is restricted to ultrasmall nanoparticles less than 6 nm in diameter, whose EPR tumor accumulation effect tends to be weak [230]. Larger nanoparticles exhibit a stronger EPR effect but require RES clearance, resulting in lower clearance efficiency. Therefore, MPN nanocomponents that efficiently accumulate in tumors due to the effect, and are also quickly eliminated through the kidneys, represent an optimal platform for treating tumors. In this context, Wang et al., synthesized multifunctional nanoparticles (FeTNPs) by combining Fe^{III} , TA, and poly(glutamic acid)-graft-methoxypoly(ethylene glycol) (PLG-g-mPEG) under specific conditions (Fig. 12A) [218]. The FeTNPs, owing to their greater molecular size, efficiently accumulated in tumor tissue through the EPR effect, thus imparting imaging capabilities. Furthermore, the FeTNPs were able to dynamically disassemble into extremely small nanoparticles when exposed to deferoxamine (DFO), allowing for rapid renal clearance (Fig. 12B). As depicted in Fig. 6B, C, the liver iron content in DFO-injected mice was significantly lower than that in mice without DFO injection, whereas the kidney iron content in DFO-injected mice was markedly elevated, reaching up to fivefold that of mice without

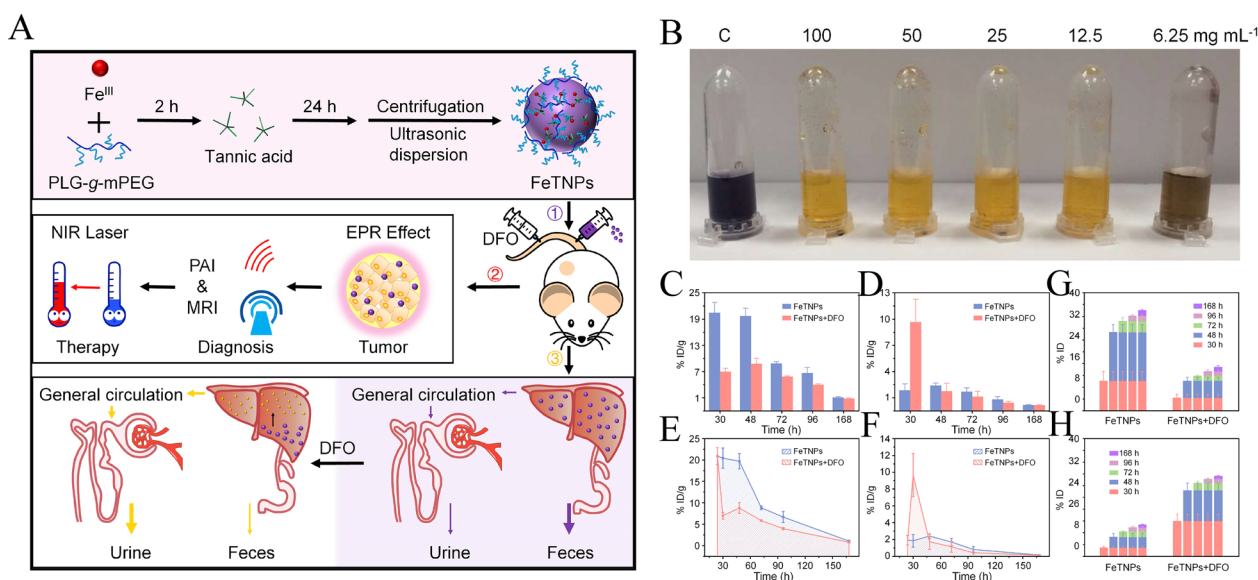


Fig. 12 The disassembling and excretion of the MPNs. **A** The schematic illustration of theranostic application and dynamic disassembling of FeTNPs. **B** The picture of FeTNPs disassembled by DFO at different concentrations. **C** The Fe content in the liver and **(D)** kidney of FeTNPs injected mice with or without injection of DFO over time. **E** The values of AUC in the mice liver and **(F)** kidney. **G** The detected Fe in feces and **(H)** urine of FeTNPs injected mice with or without injection of DFO. Reproduced with permission from Ref. [218]. Copyright 2019, Elsevier

DFO injection. These findings suggest that DFO-induced disassembly may shift the clearance pathway from hepatobiliary to renal, potentially attenuating long-term liver damage. The AUC analysis revealed that in mice without DFO injection, liver AUC was 2.2 times higher than in DFO-injected mice within 48 h post-injection, indicating accelerated liver clearance (Fig. 12E). Conversely, kidney AUC in DFO-injected mice was 2.8 times higher, suggesting predominant renal clearance (Fig. 12F). In Fig. 13G, H, fecal iron levels were notably higher in mice without DFO injection, indicating hepatic clearance of FeTNPs without DFO. Conversely, DFO-injected mice exhibited elevated urinary iron levels, suggesting renal clearance of disassembled FeTNPs with DFO. Similarly, Xu et al., constructed an MPN platform (FeAP-NPs) with a diameter of 65 nm using Fe^{III} , ACN, and PLG-g-mPEG for the purposes of tumor imaging and photothermal therapy [134]. The FeAP-NPs exhibited potent MRI imaging capabilities, while also demonstrating capacity for photothermal conversion. Furthermore, the FeAP-NPs had the ability to undergo dynamic disassembly when exposed to DFO, resulting in a transition from RES clearance to renal clearance. Consequently, the FeAP-NPs were able to eliminate tumors under PA and MRI guidance through PTT while being rapidly eliminated via renal excretion. Conversely, mucociliary clearance comprises the primary excretion method for inhaled nanoparticles.

In general, the elimination of MPN nanosystems is influenced by various factors, such as the type of material, the size of the particles, and any alterations made to the surface. The elimination of MPN nanosystems poses a

dual challenge for the body; early elimination can diminish the therapeutic benefits of MPNs, whereas delayed elimination can heighten toxicity. Hence, it is imperative to delve deeper into the intricate metabolic mechanisms of MPNs within the body to devise an optimal nanotherapeutic platform for MPNs.

Summary and prospect

The current review provides a comprehensive overview of the structural elements, synthetic techniques, functional characteristics, applications in nanomedicine, and distribution within living organisms of MPNs. Accordingly, the structure, functionality, and specific uses of representative phenols and metal ions is first discussed. Phenols, which are typically categorized into natural and synthetic phenols, have been extensively researched in various biomedical fields due to their exceptional properties [231–236]. Additionally, metal ions are essential nutrients for the human body and frequently serve as the basis for creating materials with optimal characteristics [237–239]. MPNs integrate the functions of both components, thereby providing a novel avenue for the advancement of multifunctional nanoplateforms.

The synthesis of MPNs primarily includes direct self-assembly, template self-assembly, emulsion-based assembly, and other assembly methods. Depending on the external conditions during the assembly process, MPNs can take the form of particles, nanoparticles, nano-coatings, capsules, hydrogels, etc., for use in nanomedicine. Nanoparticles are the most common form of MPNs post-synthesis, with most methods being one-step

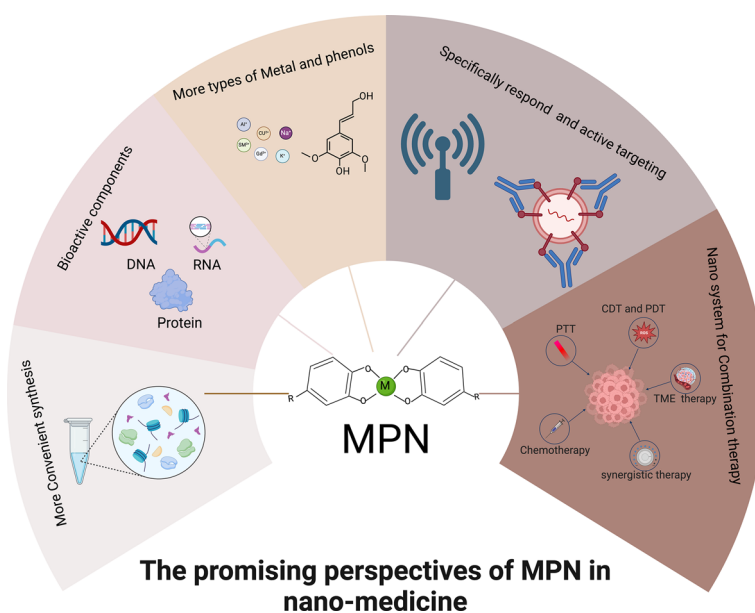


Fig. 13 The promising perspectives of MPNs in nanomedicine. This figure was drawn by biorender.com

syntheses [108, 240, 241]. Due to the adhesive properties of phenols, another common application of MPNs is in nano-coatings and films, which are primarily used for antibacterial, antifungal, substance separation, and even hair dyeing applications [25, 242–244]. The hollow capsule form of MPNs, with its excellent stimulus responsiveness and drug loading capacity, is often used in disease treatment as a carrier for nanomedicines [101, 152, 245–247]. Owing to the polyhydroxylated structure of MPNs, they can also function through the formation of hydrogels. For example, Rahim et al. found that TA and group IVB metal $\text{Ti}^{\text{IV}+}$ could form supramolecular gels in specific solvents [148]. Sun et al. developed an MPN gel to protect probiotics used in the treatment of infected wounds [248]. Experiments in vitro and in vivo showed that the MPN hydrogel could support the survival of probiotics in the presence of antibiotics, thus accelerating wound healing.

Synthesized MPNs possess numerous excellent functional characteristics, such as adhesive properties, photothermal conversion, stimulus responsiveness, and lysosomal escape. Based on these traits, MPNs have been extensively studied in fields such as cancer diagnosis and treatment [160, 188, 249–252], antimicrobial applications [253–255] and inflammatory diseases [256, 257]. In addition to the applications of MPNs in nanomedicine, other key areas of concern include the fate of MPNs in the body and their biosafety. The journey of nanomaterials in the body often follows the ADME principles [205]. After entering the body through various exposure routes, MPNs are distributed to different parts of the body. MPNs then undergo decomposition and metabolism while exerting their effects. Finally, most components of MPNs are excreted via different routes, while a small fraction may accumulate in the body's organs [31]. Balancing the targeted accumulation of MPNs in lesioned areas with the body's effective clearance of MPNs is crucial in applying MPNs in the field of nanomedicine.

Despite the growing body of research on MPNs within the field of nanomedicine [258–261], there remains a significant gap before clinical translation can be achieved. The current state of research on MPNs is characterized by several limitations and deficiencies, which include: (1) The origins and mechanisms behind certain functional properties of MPNs are unclear. For instance, only some MPNs (e.g., those based on $\text{Fe}^{\text{III}+}$, $\text{Ru}^{\text{III}+}$, $\text{V}^{\text{III}+}$) possess an extensive light absorption spectrum, while others have weaker capabilities [78]; (2) The specific relationship between the structure of MPNs and their functionality has yet to be elucidated. Understanding this relationship will aid in better balancing MPN functions against potential toxicity and in identifying the optimal

metal-phenol ratios; (3) The mechanisms by which the physicochemical properties of metal ions influence the stimulus responsiveness and stability of MPNs are not fully understood; different metal ions can affect many characteristics of MPNs, but the underlying mechanisms are yet to be unpacked; (4) The long-term carcinogenicity, teratogenicity, and other potential hazards of MPNs in humans are not clear; as most in vivo studies have been limited to mouse models without long-term follow-up, the long-term risks associated with MPNs require further investigation.

The future development trends for MPNs can be identified as follows: (1) Development of simpler, more convenient, and greener synthesis methods, which are foundational for the clinical translation and large-scale industrial production of nanomaterials; (2) Expansion of the selection range of phenols and metal ions in MPNs, as these are the primary sources of MPN functions, and different types can have variable functionalities. Thus, exploring a broader range of metal ions and phenol types will assist in developing more ideal MPNs; (3) Integration of MPNs with bioactive components (DNA, RNA, proteins) [262–264] or including di-metal and multi-metal components within MPNs [265, 266]. The combination of MPNs with bioactive components has the potential to endow MPNs with new functions and possibilities. Compared to mono-metal MPNs, multi-metal MPNs possess a greater array of functions and properties, thereby enhancing therapeutic effects; (4) Improvement of the active targeting of MPNs. Future research will focus on the combination of MPNs with active targeting moieties such as hyaluronic acid, folic acid, antibodies, etc., to form MPNs with active targeting properties [104]. (5) Development of intelligent MPN nano systems that specifically respond to the disease microenvironment. Such MPN nano systems are designed to reduce toxic side effects in systemic circulation and to increase therapeutic efficacy [255]. (6) Utilization of MPNs as multifunctional nanoplateforms for combination therapy. The high plasticity of MPNs allows for the simultaneous integration of different therapeutic methods, thereby exerting synergistic effects (Fig. 13) [165, 213].

To summarize, the unique functional properties of MPNs make them highly promising for various applications in the field of nanomedicine. If the identified limitations of MPNs are resolved in the future, MPNs have the potential to become an essential component of nanomedicine. This review comprehensively collates and condenses the existing research on MPNs, with the aim of offering guidance and establishing a foundation for future research and clinical application of MPNs.

Abbreviations

| | |
|-------------------------------|---------------------------------------|
| ACN | Anthocyanins |
| EC | Epicatechin |
| ECG | Epicatechin gallate |
| EGCG | Epigallocatechin gallate |
| TA | Tannic acid |
| MPNs | Metal-Polyphenol Networks |
| MOFs | Metal Organic Frameworks |
| ROS | Reactive oxygen species |
| DOX | Doxorubicin |
| EA | Ellagic acid |
| GA | Gallic acid |
| PEG | Polyethylene glycol |
| CaCO ₃ | Calcium carbonate |
| GSH | Glutathione |
| ATP | Adenosine triphosphate |
| TME | Tumor Microenvironment |
| H ₂ O ₂ | Hydrogen peroxide |
| MSNs | Mesoporous silica nanoparticles |
| CDT | Chemo dynamic therapy |
| PDT | Photodynamic therapy |
| PTT | Photothermal therapy |
| HMME | Haematoporphyrin monomethyl ether |
| PTCAs | Photothermal conversion agents |
| ERS | Endoplasmic reticulum stress |
| BLM | Bleomycin |
| OA | Osteoarthritis |
| PAD | Peripheral artery disease |
| PAI | Optical imaging |
| ICG | Indo-cyanine green |
| Aβ | Amyloid β-peptide |
| Gel | Gelatin |
| EPR | Enhanced permeability and retention |
| RES | Reticuloendothelial system |
| DFO | Deferoxamine |
| Q-NPs | Quercetin-based MPN nanoparticles |
| MRI | Magnetic Resonance Imaging |
| PET | Position Emission Computed Tomography |

Acknowledgements

Not applicable.

Author contributions

Zhengming Tang: Conceptualization; Writing—original draft; Zhijie Hang and Shengyi Huang: Methodology; Mingshu Huang and Hongyu Liu: Visualization; Bo Jia and Jianzhong Du: Writing—review and editing; All authors have agreed to the published version of the manuscript.

Funding

This work was jointly supported by the program of Stomatological Hospital, School of Stomatology, Southern Medical University (PY2022015), the Guangdong Provincial Medical Science and Technology Research Fund Project (B2023413), the Guangdong Provincial Key Areas Special Project for General Universities (Biomedicine and Health, 2023ZDZX2009), National natural science foundation of China (22335005), Innovation Program of Shanghai Municipal Education Commission (2023ZKZD28) and Guangdong Provincial Administration of Traditional Chinese Medicine Scientific Research General Project (20251265). Open access funding provided by Stomatological Hospital, School of Stomatology, Southern Medical University.

Availability of data and materials

No datasets were generated or analysed during the current study.

Declarations

Ethics approval and consent to participate

Not applicable.

Consent for publication

All authors have agreed to the published version of the manuscript.

Competing interests

The authors declare no competing interests.

Author details

¹Stomatological Hospital, School of Stomatology, Southern Medical University, Guangzhou, China. ²Yuexiu District Stomatological Hospital, Guangzhou, Guangdong, China. ³Department of Gynaecology and Obstetrics, Shanghai Key Laboratory of Anesthesiology and Brain Functional Modulation, Clinical Research Center for Anesthesiology and Perioperative Medicine, School of Medicine, Translational Research Institute of Brain and Brain-Like Intelligence, Shanghai Fourth People's Hospital, Tongji University, Shanghai 200434, China. ⁴Department of Polymeric Materials, School of Materials Science and Engineering, Key Laboratory of Advanced Civil Engineering Materials of Ministry of Education, Tongji University, 4800 Caoan Road, Shanghai 201804, China.

Received: 5 September 2024 Accepted: 9 February 2025

Published online: 02 March 2025

References

1. Fadeel B. Nanomedicine: towards innovative solutions in the clinic. *J Intern Med*. 2021;290(3):746–8.
2. Choi YH, Han HK. Nanomedicines: current status and future perspectives in aspect of drug delivery and pharmacokinetics. *J Pharm Investig*. 2018;48(1):43–60.
3. Abdel-Mageed HM, et al. Nanoparticles in nanomedicine: a comprehensive updated review on current status, challenges and emerging opportunities. *J Microencapsul*. 2021;38(6):414–36.
4. Bakuzis AF. Nanomedicine and thermal therapies: where are we going? *Int J Hyperthermia*. 2020;37(3):1–3.
5. Calzoni E, et al. Biocompatible polymer nanoparticles for drug delivery applications in cancer and neurodegenerative disorder therapies. *J Funct Biomater*. 2019. <https://doi.org/10.3390/jfb10010004>.
6. Mostafa E, et al. *Centaurea pumilio* L. extract and nanoparticles: a candidate for healthy skin. *Colloids Surf B Biointerfaces*. 2019;182:110350.
7. Moghimi SM, Hunter AC, Murray JC. Long-circulating and target-specific nanoparticles: theory to practice. *Pharmacol Rev*. 2001;53(2):283–318.
8. Patra JK, et al. Nano based drug delivery systems: recent developments and future prospects. *J Nanobiotechnol*. 2018;16(1):71.
9. Watkins R, et al. Natural product-based nanomedicine: recent advances and issues. *Int J Nanomed*. 2015;10:6055–74.
10. Wu LP, Wang D, Li Z. Grand challenges in nanomedicine. *Mater Sci Eng C Mater Biol Appl*. 2020;106:110302.
11. Yang C, Merlin D. Challenges to safe nanomedicine treatment. *Nanomaterials*. 2023. <https://doi.org/10.3390/nano13071171>.
12. Quideau S, et al. Plant polyphenols: chemical properties, biological activities, and synthesis. *Angew Chem Int Ed Engl*. 2011;50(3):586–621.
13. Papuc C, et al. Plant polyphenols as antioxidant and antibacterial agents for shelf-life extension of meat and meat products: classification, structures, sources, and action mechanisms. *Compr Rev Food Sci Food Saf*. 2017;16(6):1243–68.
14. Li J, et al. Versatile surface engineering of porous nanomaterials with bioinspired polyphenol coatings for targeted and controlled drug delivery. *Nanoscale*. 2016;8(16):8600–6.
15. Sileika TS, et al. Colorless multifunctional coatings inspired by polyphenols found in tea, chocolate, and wine. *Angew Chem Int Ed Engl*. 2013;52(41):10766–70.
16. Panchatcharam M, et al. Curcumin improves wound healing by modulating collagen and decreasing reactive oxygen species. *Mol Cell Biochem*. 2006;290(1–2):87–96.
17. Merrell JG, et al. Curcumin-loaded poly(epsilon-caprolactone) nanofibers: diabetic wound dressing with anti-oxidant and anti-inflammatory properties. *Clin Exp Pharmacol Physiol*. 2009;36(12):1149–56.
18. Ejima H, Richardson JJ, Caruso F. Metal-phenolic networks as a versatile platform to engineer nanomaterials and biointerfaces. *Nano Today*. 2017;12:136–48.
19. Ejima H, et al. One-step assembly of coordination complexes for versatile film and particle engineering. *Science*. 2013;341(6142):154–7.

20. Dai Y, et al. Hypochlorous acid promoted platinum drug chemotherapy by myeloperoxidase-encapsulated therapeutic metal phenolic nanoparticles. *ACS Nano*. 2018;12(1):455–63.
21. Ghafarifar F, et al. Fe₃O₄@Bio-MOF nanoparticles combined with artemisinin, glucantime®, or shark cartilage extract on Iranian strain of *Leishmania major* (MRHO/IR/75/ER): an in-vitro and in-vivo study. *Iran J Parasitol*. 2020;15(4):537–48.
22. Fu LQ, et al. Surface engineered metal-organic frameworks (MOFs) based novel hybrid systems for effective wound healing: a review of recent developments. *Front Bioeng Biotechnol*. 2020;8:576348.
23. Yang M, et al. Recent advances in metal-organic framework-based materials for anti-staphylococcus aureus infection. *Nano Res*. 2022;15(7):6220–42.
24. Zhang Y, et al. Metal-phenolic network coatings for engineering bioactive interfaces. *Colloids Surf, B*. 2021;205:111851.
25. Wang R, et al. Superwetting oil/water separation membrane constructed from in situ assembled metal-phenolic networks and metal-organic frameworks. *ACS Appl Mater Interfaces*. 2020;12(8):10000–8.
26. Liang H, et al. Supramolecular design and applications of polyphenol-based architecture: A review. *Adv Colloid Interface Sci*. 2019;272:102019.
27. Zhang C, et al. Interfacing metal-polyphenolic networks upon photo-thermal gold nanorods for triplex-evolved biocompatible bactericidal activity. *J Hazard Mater*. 2022;426:127824.
28. Kim T, et al. A gold/silver hybrid nanoparticle for treatment and photoacoustic imaging of bacterial infection. *ACS Nano*. 2018;12(6):5615–25.
29. Lemire JA, Harrison JJ, Turner RJ. Antimicrobial activity of metals: mechanisms, molecular targets and applications. *Nat Rev Microbiol*. 2013;11(6):371–84.
30. Li Y, et al. Recent advances in the development and antimicrobial applications of metal-phenolic networks. *Adv Sci*. 2022;9(27):e2202684.
31. Zhang Z, et al. Recent advances in metal-phenolic networks for cancer theranostics. *Small*. 2021;17(43):e2100314.
32. Chen W, et al. Recent advances of Fe(III)/Fe(II)-MPNs in biomedical applications. *Pharmaceutics*. 2023. <https://doi.org/10.3390/pharmaceutics15051323>.
33. Guo Z, et al. Tannic acid-based metal phenolic networks for bio-applications: a review. *J Mater Chem B*. 2021;9(20):4098–110.
34. Zhou Y, et al. Natural polyphenols for prevention and treatment of cancer. *Nutrients*. 2016. <https://doi.org/10.3390/nu8080515>.
35. Olszowy M. What is responsible for antioxidant properties of polyphenolic compounds from plants? *Plant Physiol Biochem*. 2019;144:135–43.
36. Dini I, Grumetto L. Recent advances in natural polyphenol research. *Molecules*. 2022. <https://doi.org/10.3390/molecules27248777>.
37. Khan N, Mukhtar H. Tea polyphenols for health promotion. *Life Sci*. 2007;81(7):519–33.
38. Khan N, Mukhtar H. Tea polyphenols in promotion of human health. *Nutrients*. 2018. <https://doi.org/10.3390/nu11010039>.
39. Yang CS, et al. Cancer prevention by tea: animal studies, molecular mechanisms and human relevance. *Nat Rev Cancer*. 2009;9(6):429–39.
40. Peter B, Bosze S, Horvath R. Biophysical characteristics of proteins and living cells exposed to the green tea polyphenol epigallocatechin-3-gallate (EGCG): review of recent advances from molecular mechanisms to nanomedicine and clinical trials. *Eur Biophys J*. 2017;46(1):1–24.
41. Bendokas V, et al. Anthocyanins: from the field to the antioxidants in the body. *Antioxidants*. 2020. <https://doi.org/10.3390/antiox9090819>.
42. de Arruda Nascimento E, et al. In vitro anticancer properties of anthocyanins: a systematic review. *Biochim Biophys Acta Rev Cancer*. 2022;1877(4):188748.
43. Durazzo A, et al. Polyphenols: a concise overview on the chemistry, occurrence, and human health. *Phytother Res*. 2019;33(9):2221–43.
44. Xu Y, et al. Tannic acid attenuated irradiation-induced apoptosis in megakaryocytes. *Exp Cell Res*. 2018;370(2):409–16.
45. Youness RA, et al. Recent advances in tannic acid (gallotannin) anticancer activities and drug delivery systems for efficacy improvement; a comprehensive review. *Molecules*. 2021. <https://doi.org/10.3390/molecules26051486>.
46. Chen MC, et al. Tannic acid attenuate AKT phosphorylation to inhibit UMC3 bladder cancer cell proliferation. *Mol Cell Biochem*. 2022;477(12):2863–9.
47. Sathishkumar G, et al. Recent progress in tannic acid-driven anti-bacterial/antifouling surface coating strategies. *J Mater Chem B*. 2022;10(14):2296–315.
48. Wang Y, et al. Quercetin alleviates acute kidney injury by inhibiting ferroptosis. *J Adv Res*. 2021;28:231–43.
49. Minaei A, et al. Co-delivery with nano-quercetin enhances doxorubicin-mediated cytotoxicity against MCF-7 cells. *Mol Biol Rep*. 2016;43(2):99–105.
50. Suksiriworapong J, et al. Comparison of poly(ϵ -caprolactone) chain lengths of poly(ϵ -caprolactone)-co-d- α -tocopheryl-poly(ethylene glycol) 1000 succinate nanoparticles for enhancement of quercetin delivery to SKBR3 breast cancer cells. *Eur J Pharm Biopharm*. 2016;101:15–24.
51. Patel RV, et al. Therapeutic potential of quercetin as a cardiovascular agent. *Eur J Med Chem*. 2018;155:889–904.
52. Renaud S, de Lorgeril M. Wine, alcohol, platelets, and the French paradox for coronary heart disease. *Lancet*. 1992;339(8808):1523–6.
53. Vestergaard M, Ingmer H. Antibacterial and antifungal properties of resveratrol. *Int J Antimicrob Agents*. 2019;53(6):716–23.
54. Bhattarai G, et al. Resveratrol prevents alveolar bone loss in an experimental rat model of periodontitis. *Acta Biomater*. 2016;29:398–408.
55. Rauf A, et al. Resveratrol as an anti-cancer agent: a review. *Crit Rev Food Sci Nutr*. 2018;58(9):1428–47.
56. Ji Q, et al. Resveratrol suppresses epithelial-to-mesenchymal transition in colorectal cancer through TGF- β 1/Smads signaling pathway mediated Snail/E-cadherin expression. *BMC Cancer*. 2015;15:97.
57. Akbik D, et al. Curcumin as a wound healing agent. *Life Sci*. 2014;116(1):1–7.
58. Gan RY, et al. Absorption, metabolism, anti-cancer effect and molecular targets of epigallocatechin gallate (EGCG): an updated review. *Crit Rev Food Sci Nutr*. 2018;58(6):924–41.
59. Sarfraz A, et al. Hispolon: a natural polyphenol and emerging cancer killer by multiple cellular signaling pathways. *Environ Res*. 2020;190:110017.
60. Zeng Y, et al. Natural product gossypol and its derivatives in precision cancer medicine. *Curr Med Chem*. 2019;26(10):1849–73.
61. Zeb A. Ellagic acid in suppressing in vivo and in vitro oxidative stresses. *Mol Cell Biochem*. 2018;448(1–2):27–41.
62. Wang J, et al. Ellagic acid from hull blackberries: extraction, purification, and potential anticancer activity. *Int J Mol Sci*. 2023. <https://doi.org/10.3390/ijms242015228>.
63. Bai J, et al. Gallic acid: pharmacological activities and molecular mechanisms involved in inflammation-related diseases. *Biomed Pharmacother*. 2021;133:110985.
64. Chen L, Cao H, Xiao J. 2 Polyphenols absorption, bioavailability, and metabolomics. In: Galanakis C, editor. *Polyphenols: properties, recovery, and applications*. Amsterdam: Elsevier; 2018. p. 45–67.
65. Bohn T, et al. Mind the gap-deficits in our knowledge of aspects impacting the bioavailability of phytochemicals and their metabolites—a position paper focusing on carotenoids and polyphenols. *Mol Nutr Food Res*. 2015;59(7):1307–23.
66. Lewandowska U, Fichna J, Górlach S. Enhancement of anticancer potential of polyphenols by covalent modifications. *Biochem Pharmacol*. 2016;109:1–13.
67. Lee UJ, et al. Recent trends in the modification of polyphenolic compounds using hydroxylation and glycosylation. *Curr Opin Biotechnol*. 2023;80:102914.
68. Jeong JH, et al. Surface camouflage of pancreatic islets using 6-arm-PEG-catechol in combined therapy with tacrolimus and anti-CD154 monoclonal antibody for xenotransplantation. *Biomaterials*. 2011;32(31):7961–70.
69. Shin JM, et al. Metal-phenolic network-coated hyaluronic acid nanoparticles for pH-responsive drug delivery. *Pharmaceutics*. 2019. <https://doi.org/10.3390/pharmaceutics11120636>.
70. Liang J, Jiang D, Noble PW. Hyaluronan as a therapeutic target in human diseases. *Adv Drug Deliv Rev*. 2016;97:186–203.
71. Su J, et al. Catechol polymers for pH-responsive, targeted drug delivery to cancer cells. *J Am Chem Soc*. 2011;133(31):11850–3.
72. Budzisz E. Role of metal ions complexes and their ligands in medicine, pharmacy and cosmetology. *Curr Med Chem*. 2019;26(4):578–9.
73. Thompson KH, Orvig C. Boon and bane of metal ions in medicine. *Science*. 2003;300(5621):936–9.

74. Li S, et al. Application of bioactive metal ions in the treatment of bone defects. *J Mater Chem B*. 2022;10(45):9369–88.
75. Kargozar S, et al. Bioactive glasses: sprouting angiogenesis in tissue engineering. *Trends Biotechnol*. 2018;36(4):430–44.
76. Gao P, et al. Biofunctional magnesium coated Ti6Al4V scaffold enhances osteogenesis and angiogenesis in vitro and in vivo for orthopedic application. *Bioact Mater*. 2020;5(3):680–93.
77. Liu T, et al. Ferrous-supply-regeneration nanoengineering for cancer-cell-specific ferroptosis in combination with imaging-guided photodynamic therapy. *ACS Nano*. 2018;12(12):12181–92.
78. Liu T, et al. Metal ion/tannic acid assembly as a versatile photothermal platform in engineering multimodal nanotheranostics for advanced applications. *ACS Nano*. 2018;12(4):3917–27.
79. Geng H, et al. Metal ion-directed functional metal-phenolic materials. *Chem Rev*. 2022;122(13):1432–73.
80. Dougherty DA. Cation- π interactions in chemistry and biology: a new view of benzene, Phe, Tyr, and Trp. *Science*. 1996;271(5246):163–8.
81. Mahadevi AS, Sastry GN. Cation- π interaction: its role and relevance in chemistry, biology, and material science. *Chem Rev*. 2013;113(3):2100–38.
82. Wei F, et al. In situ facile loading of noble metal nanoparticles on polydopamine nanospheres via galvanic replacement reaction for multifunctional catalysis. *Sci China Chem*. 2017;60(9):1236–42.
83. Kim J, et al. Photochemically enhanced selective adsorption of gold ions on tannin-coated porous polymer microspheres. *ACS Appl Mater Interfaces*. 2019;11(24):21915–25.
84. Liu Y, Ai K, Lu L. Polydopamine and its derivative materials: synthesis and promising applications in energy, environmental, and biomedical fields. *Chem Rev*. 2014;114(9):5057–115.
85. Can M. Reduction of palladium onto pyrogallol-derived nano-resin and its mechanism. *Chem Eng J*. 2015. <https://doi.org/10.1016/j.cej.2015.04.041>.
86. Kumar K, Mandal B, Tammina DSK. Green synthesis of nano platinum using naturally occurring polyphenols. *RSC Adv*. 2013;3:4033–9.
87. Guo L, et al. A mussel-inspired polydopamine coating as a versatile platform for the in situ synthesis of graphene-based nanocomposites. *Nanoscale*. 2012;4:5864–7.
88. Hartmann D, et al. The structure of Bis(catecholato)silanes: phase adaptation by dynamic covalent chemistry of the Si-O bond. *J Am Chem Soc*. 2021;143(44):18784–93.
89. Mu M, et al. Chitosan coated pH-responsive metal-polyphenol delivery platform for melanoma chemotherapy. *Carbohydr Polym*. 2021;264:118000.
90. Hao L, et al. Novel porous Fe(3)O(4)@C nanocomposite from magnetic metal-phenolic networks for the extraction of chlorophenols from environmental samples. *Talanta*. 2019;194:673–9.
91. Tao G, et al. Manganese-phenolic networks coated black phosphorus nanosheets for theranostics combining magnetic resonance/photoacoustic dual-modal imaging and photothermal therapy. *Chem Commun*. 2018. <https://doi.org/10.1039/c8cc08833k>.
92. Bartzoka ED, et al. Coordination complexes and one-step assembly of lignin for versatile nanocapsule engineering. *ACS Sustain Chem Eng*. 2016;4(10):5194–203.
93. Bertleff-Zieschang N, et al. Biofunctional metal-phenolic films from dietary flavonoids. *Chem Commun*. 2017;53(6):1068–71.
94. Pan S, et al. Modular assembly of host-guest metal-phenolic networks using macrocyclic building blocks. *Angew Chem Int Ed Engl*. 2020;59(1):275–80.
95. Rahim MA, et al. Surface-confined amorphous films from metal-coordinated simple phenolic ligands. *Chem Mater*. 2015;27:5825–32.
96. Park C, et al. Signal-induced release of guests from a photolabile metal-phenolic supramolecular cage and its hybrid assemblies. *Angew Chem Int Ed Engl*. 2017;56(20):5485–9.
97. Zhang L, et al. An adenosine triphosphate-responsive autocatalytic fenton nanoparticle for tumor ablation with self-supplied H₂O₂ and acceleration of Fe(III)/Fe(II) conversion. *Nano Lett*. 2018;18(12):7609–18.
98. Ringwald C, Ball V. Layer-by-layer deposition of tannic acid and Fe³⁺ cations is of electrostatic nature but almost ionic strength independent at pH 5. *J Colloid Interface Sci*. 2015;450:119–26.
99. Kim S, Kim DS, Kang SM. Reversible layer-by-layer deposition on solid substrates inspired by mussel byssus cuticle. *Chem Asian J*. 2014;9(1):63–6.
100. Rahim MA, et al. Coordination-driven multistep assembly of metal-polyphenol films and capsules. *Chem Mater*. 2014;26(4):1645–53.
101. Guo J, et al. Engineering multifunctional capsules through the assembly of metal-phenolic networks. *Angew Chem Int Ed Engl*. 2014;53(22):5546–51.
102. Rahim MA, et al. Rust-mediated continuous assembly of metal-phenolic networks. *Adv Mater*. 2017. <https://doi.org/10.1002/adma.201606717>.
103. Guo J, et al. Modular assembly of superstructures from polyphenol-functionalized building blocks. *Nat Nanotechnol*. 2016;11(12):1105–11.
104. Ju Y, et al. Engineered Metal-phenolic capsules show tunable targeted delivery to cancer cells. *Biomacromol*. 2016;17(6):2268–76.
105. Ping Y, et al. pH-Responsive capsules engineered from metal-phenolic networks for anticancer drug delivery. *Small*. 2015;11(17):2032–6.
106. Shen G, et al. Interfacial cohesion and assembly of bioadhesive molecules for design of long-term stable hydrophobic nanodrugs toward effective anticancer therapy. *ACS Nano*. 2016;10(6):5720–9.
107. La Y, et al. Templated synthesis of cubic crystalline single networks having large open-space lattices by polymer cubosomes. *Nat Commun*. 2018;9(1):5327.
108. Lin Z, et al. Ordered mesoporous metal-phenolic network particles. *J Am Chem Soc*. 2020;142(1):335–41.
109. Hörmann K, Zimmer A. Drug delivery and drug targeting with parental lipid nanoemulsions - A review. *J Control Release*. 2016;223:85–98.
110. Wang H, et al. Applications of metal-phenolic networks in nanomedicine: a review. *Biomater Sci*. 2022;10(20):5786–808.
111. Besford QA, et al. Self-assembled metal-phenolic networks on emulsions as low-fouling and pH-responsive particles. *Small*. 2018;14(39):e1802342.
112. Wu D, et al. Pickering emulsion stabilized by metal-phenolic architectures: a straightforward in situ assembly strategy. *J Agric Food Chem*. 2021;69(39):11709–19.
113. Dai Y, et al. Self-assembled nanoparticles from phenolic derivatives for cancer therapy. *Adv Healthc Mater*. 2017. <https://doi.org/10.1002/adhm.201700467>.
114. Wei J, et al. Sol-gel synthesis of metal-phenolic coordination spheres and their derived carbon composites. *Angew Chem Int Ed Engl*. 2018;57(31):9838–43.
115. Maerten C, et al. Electrotriggered confined self-assembly of metal-polyphenol nanocoatings using a morphogenic approach. *Chem Mater*. 2017;29(22):9668–79.
116. Hong S, et al. Pyrogallol 2-aminoethane: a plant flavonoid-inspired molecule for material-independent surface chemistry. *Adv Mater Interfaces*. 2014;1(4):1400113.
117. Harrington MJ, et al. Iron-clad fibers: a metal-based biological strategy for hard flexible coatings. *Science*. 2010;328(5975):216–20.
118. Wilker JJ. The iron-fortified adhesive system of marine mussels. *Angew Chem Int Ed*. 2010;49(44):8076–8.
119. Siebert KJ, Troukhanova NV, Lynn PY. Nature of polyphenol–protein interactions. *J Agric Food Chem*. 1996;44(1):80–5.
120. Liang H, et al. Engineering multifunctional films based on metal-phenolic networks for rational pH-responsive delivery and cell imaging. *ACS Biomater Sci Eng*. 2016;2(3):317–25.
121. Ozawa H, Haga MA. Soft nano-wrapping on graphene oxide by using metal-organic network films composed of tannic acid and Fe ions. *Phys Chem Chem Phys*. 2015;17(14):8609–13.
122. Park JH, et al. A cytoprotective and degradable metal-polyphenol nanoshell for single-cell encapsulation. *Angew Chem Int Ed Engl*. 2014;53(46):12420–5.
123. Xie L, et al. Engineering metal-phenolic networks for enhancing cancer therapy by tumor microenvironment modulation. *Wiley Interdiscip Rev Nanomed Nanobiotechnol*. 2023;15(3):e1864.
124. Cherrak SA, et al. In vitro antioxidant versus metal ion chelating properties of flavonoids: a structure-activity investigation. *PLoS ONE*. 2016;11(10):e0165575.
125. Perron NR, et al. Kinetics of iron oxidation upon polyphenol binding. *Dalton Trans*. 2010;39(41):9982–7.

126. Luo C, et al. Self-assembled redox dual-responsive prodrug-nanosystem formed by single thioether-bridged paclitaxel-fatty acid conjugate for cancer chemotherapy. *Nano Lett.* 2016;16(9):5401–8.
127. Dong J, et al. Facile, smart, and degradable metal-organic framework nanopesticides gated with Felli-tannic acid networks in response to seven biological and environmental stimuli. *ACS Appl Mater Interfaces.* 2021;13(16):19507–20.
128. Tu J, Yu ACH. Ultrasound-mediated drug delivery: sonoporation mechanisms, biophysics, and critical factors. *BME Frontiers.* 2022;2022:9807347.
129. Wang Z, et al. Metal-phenolic-network-coated dendrimer-drug conjugates for tumor MR imaging and chemo/chemodynamic therapy via amplification of endoplasmic reticulum stress. *Adv Mater.* 2022;34(7):2107009.
130. Qin J, et al. Synthesis of gadolinium/iron-bimetal-phenolic coordination polymer nanoparticles for theranostic applications. *Nanoscale.* 2020;12(10):6096–103.
131. Hessel CM, et al. Copper selenide nanocrystals for photothermal therapy. *Nano Lett.* 2011;11(6):2560–6.
132. Tian Q, et al. Hydrophilic Cu9S5 nanocrystals: a photothermal agent with a 25.7% heat conversion efficiency for photothermal ablation of cancer cells in vivo. *ACS Nano.* 2011;5(12):9761–71.
133. Zhao G, et al. Novel metal polyphenol framework for mr imaging-guided photothermal therapy. *ACS Appl Mater Interfaces.* 2018;10(4):3295–304.
134. Xu C, et al. Multifunctional theranostic nanoparticles derived from fruit-extracted anthocyanins with dynamic disassembly and elimination abilities. *ACS Nano.* 2018;12(8):8255–65.
135. Jia C, Guo Y, Wu FG. Chemodynamic therapy via fenton and fenton-like nanomaterials: strategies and recent advances. *Small.* 2022;18(6):e2103868.
136. Jia Q, et al. Rejuvenated photodynamic therapy for bacterial infections. *Adv Healthc Mater.* 2019;8(14):e1900608.
137. Brillas E, Sirés I, Oturan MA. Electro-fenton process and related electrochemical technologies based on fenton's reaction chemistry. *Chem Rev.* 2009;109(12):6570–631.
138. Wang Q, et al. Encapsulation of enzymes in metal-phenolic network capsules for the trigger of intracellular cascade reactions. *Langmuir.* 2021;37(38):11292–300.
139. Guo Y, et al. Polyphenol-containing nanoparticles: synthesis, properties, and therapeutic delivery. *Adv Mater.* 2021;33(22):e2007356.
140. Li L, et al. In situ polymerized hollow mesoporous organosilica biocatalysis nanoreactor for enhancing ROS-mediated anticancer therapy. *Adv Funct Mater.* 2020. <https://doi.org/10.1002/adfm.201907716>.
141. Behzadi S, et al. Cellular uptake of nanoparticles: journey inside the cell. *Chem Soc Rev.* 2017;46(14):4218–44.
142. Pei D, Buyanova M. Overcoming endosomal entrapment in drug delivery. *Bioconjug Chem.* 2019;30(2):273–83.
143. Coué G, Engbersen JF. Functionalized linear poly(amidoamine)s are efficient vectors for intracellular protein delivery. *J Control Release.* 2011;152(1):90–8.
144. Cohen S, et al. Bioreducible poly(amidoamine)s as carriers for intracellular protein delivery to intestinal cells. *Biomaterials.* 2012;33(2):614–23.
145. Chen J, et al. Metal-phenolic coatings as a platform to trigger endosomal escape of nanoparticles. *ACS Nano.* 2019;13(10):11653–64.
146. Menyo MS, Hawker CJ, Waite JH. Versatile tuning of supramolecular hydrogels through metal complexation of oxidation-resistant catechol-inspired ligands. *Soft Matter.* 2013. <https://doi.org/10.1039/C3SM51824H>.
147. Li Q, et al. Controlling hydrogel mechanics via bio-inspired polymer-nanoparticle bond dynamics. *ACS Nano.* 2016;10(1):1317–24.
148. Rahim MA, et al. Metal-phenolic supramolecular gelation. *Angew Chem Int Ed Engl.* 2016;55(44):13803–7.
149. Qin S-Y, Zhang A-Q, Zhang X-Z. Recent advances in targeted tumor chemotherapy based on smart nanomedicines. *Small.* 2018;14(45):1802417.
150. Wang X, et al. Recent progress of chemodynamic therapy-induced combination cancer therapy. *Nano Today.* 2020;35:100946.
151. Liu J, et al. Boosting tumor treatment by dredging the hurdles of chemodynamic therapy synergistic ion therapy. *Chem Eng J.* 2021;411:128440.
152. Wei Y, et al. pH-sensitive metal-phenolic network capsules for targeted photodynamic therapy against cancer cells. *Artif Cells Nanomed Biotechnol.* 2018;46(8):1552–61.
153. Zhang Z, et al. Polyphenol-based nanomedicine evokes immune activation for combination cancer treatment. *Angew Chem Int Ed Engl.* 2021;60(4):1967–75.
154. Jung HS, et al. Organic molecule-based photothermal agents: an expanding photothermal therapy universe. *Chem Soc Rev.* 2018;47(7):2280–97.
155. Chen WH, et al. Overcoming the heat endurance of tumor cells by interfering with the anaerobic glycolysis metabolism for improved photothermal therapy. *ACS Nano.* 2017;11(2):1419–31.
156. Yang GG, et al. Multifunctional low-temperature photothermal nanodrug with in vivo clearance, ROS-scavenging and anti-inflammatory abilities. *Biomaterials.* 2019;216:119280.
157. Albin A, Sporn MB. The tumour microenvironment as a target for chemoprevention. *Nat Rev Cancer.* 2007;7(2):139–47.
158. Liu F, et al. Targeted disruption of tumor vasculature via polyphenol nanoparticles to improve brain cancer treatment. *Cell Rep Phys Sci.* 2022. <https://doi.org/10.1016/j.xcrp.2021.100691>.
159. Sang W, et al. Oxygen-enriched metal-phenolic X-Ray nanoprocessor for cancer radio-radiodynamic therapy in combination with checkpoint blockade immunotherapy. *Adv Sci.* 2021;8(4):2003338.
160. Wang Z, et al. Metal-phenolic-network-coated dendrimer-drug conjugates for tumor MR imaging and chemo/chemodynamic therapy via amplification of endoplasmic reticulum stress. *Adv Mater.* 2022;34(7):e2107009.
161. Su Q, et al. Facile preparation of a metal-phenolic network-based lymph node targeting nanovaccine for antitumor immunotherapy. *Acta Biomater.* 2023;158:510–24.
162. Fan W, et al. Nanotechnology for multimodal synergistic cancer therapy. *Chem Rev.* 2017;117(22):13566–638.
163. Liu P, et al. Anti-PD-L1 DNAzyme loaded photothermal Mn(2+) / Fe(3+) hybrid metal-phenolic networks for cyclically amplified tumor ferroptosis-immunotherapy. *Adv Healthc Mater.* 2022;11(8):e2102315.
164. Feng W, et al. Fe(III)-shikonin supramolecular nanomedicine for combined therapy of tumor via ferroptosis and necroptosis. *Adv Healthc Mater.* 2022;11(2):e2101926.
165. Fan JX, et al. A metal-polyphenol network coated nanotheranostic system for metastatic tumor treatments. *Small.* 2017. <https://doi.org/10.1002/sml.201702714>.
166. Liu Y, et al. Tumor microenvironment-responsive theranostic nanopatform for in situ self-boosting combined phototherapy through intracellular reassembly. *ACS Appl Mater Interfaces.* 2020;12(6):6966–77.
167. Zhou L, et al. Metal-polyphenol-network coated prussian blue nanoparticles for synergistic ferroptosis and apoptosis via triggered GPX4 inhibition and concurrent in situ bleomycin toxicification. *Small.* 2021;17(47):e2103919.
168. Ge L, et al. Nanosilver particles in medical applications: synthesis, performance, and toxicity. *Int J Nanomed.* 2014;9:2399–407.
169. Chouchani ET, et al. Ischaemic accumulation of succinate controls reperfusion injury through mitochondrial ROS. *Nature.* 2014;515(7527):431–5.
170. Alomary MN, Ansari MA. Proanthocyanin-capped biogenic TiO₂(2) nanoparticles with enhanced penetration, antibacterial and ROS mediated inhibition of bacteria proliferation and biofilm formation: a comparative approach. *Chemistry.* 2021;27(18):5817–29.
171. Sun X, et al. Multifunctional chitosan-copper-gallic acid based antibacterial nanocomposite wound dressing. *Int J Biol Macromol.* 2021;167:10–22.
172. Guo S, et al. One-step synthesis of multifunctional chitosan hydrogel for full-thickness wound closure and healing. *Adv Healthc Mater.* 2022;11(4):e2101808.
173. Hu C, et al. Synergistic chemical and photodynamic antimicrobial therapy for enhanced wound healing mediated by multifunctional light-responsive nanoparticles. *Biomacromol.* 2019;20(12):4581–92.
174. Liu L, et al. Prevention of bacterial colonization based on self-assembled metal-phenolic nanocoating from rare-earth ions and catechin. *ACS Appl Mater Interfaces.* 2020;12(19):22237–45.

175. Deng H, et al. Facile and eco-friendly fabrication of polysaccharides-based nanocomposite hydrogel for photothermal treatment of wound infection. *Carbohydr Polym.* 2020;230:115565.
176. Cherepanov PV, et al. Electrochemical behavior and redox-dependent disassembly of gallic acid/Fe(III) metal-phenolic networks. *ACS Appl Mater Interfaces.* 2018;10(6):5828–34.
177. Wei H, et al. Epigallocatechin-3-gallate (EGCG) based metal-polyphenol nanoformulations alleviates chondrocytes inflammation by modulating synovial macrophages polarization. *Biomed Pharmacother.* 2023;161:114366.
178. Li Y, et al. Tannic acid/Sr(2+)-coated silk/graphene oxide-based meniscus scaffold with anti-inflammatory and anti-ROS functions for cartilage protection and delaying osteoarthritis. *Acta Biomater.* 2021;126:119–31.
179. Narula N, Olin JW, Narula N. Pathologic disparities between peripheral artery disease and coronary artery disease. *Arterioscler Thromb Vasc Biol.* 2020;40(9):1982–9.
180. Duan J, et al. Construction and application of therapeutic metal-polyphenol capsule for peripheral artery disease. *Biomaterials.* 2020;255:120199.
181. Vimalraj S, et al. Kaempferol-zinc(II) complex synthesis and evaluation of bone formation using zebrafish model. *Life Sci.* 2020;256:117993.
182. Lee S, et al. Surface engineering of titanium alloy using metal-polyphenol network coating with magnesium ions for improved osseointegration. *Biomater Sci.* 2020;8(12):3404–17.
183. Zhang Y, et al. Metal phenolic nanodressing of porous polymer scaffolds for enhanced bone regeneration via interfacial gating growth factor release and stem cell differentiation. *ACS Appl Mater Interfaces.* 2022;14(1):268–77.
184. Zheng G, Li S. Medical image computing in diagnosis and intervention of spinal diseases. *Comput Med Imaging Graph.* 2015;45:99–101.
185. Alnazer I, et al. Recent advances in medical image processing for the evaluation of chronic kidney disease. *Med Image Anal.* 2021;69:101960.
186. Xie W, et al. Metal-phenolic networks: facile assembled complexes for cancer theranostics. *Theranostics.* 2021;11(13):6407–26.
187. Ahrens ET, Bulte JW. Tracking immune cells in vivo using magnetic resonance imaging. *Nat Rev Immunol.* 2013;13(10):755–63.
188. Zhang Y, et al. Versatile metal-phenolic network nanoparticles for multitargeted combination therapy and magnetic resonance tracing in glioblastoma. *Biomaterials.* 2021;278:121163.
189. Guo J, et al. Nanoporous metal-phenolic particles as ultrasound imaging probes for hydrogen peroxide. *Adv Healthc Mater.* 2015;4(14):2170–5.
190. Wang X, et al. Polyphenol-poloxamer self-assembled supramolecular nanoparticles for tumor NIRF/PET imaging. *Adv Healthc Mater.* 2018;7(15):e1701505.
191. Foray C, et al. Multimodal molecular imaging of the tumour microenvironment. *Adv Exp Med Biol.* 2020;1225:71–87.
192. Wang J, et al. Polyphenol-based nanopatform for MRI/PET dual-modality imaging guided effective combination chemotherapy. *J Mater Chem B.* 2019;7(37):5688–94.
193. Hu D, et al. Indocyanine green-loaded polydopamine-iron ions coordination nanoparticles for photoacoustic/magnetic resonance dual-modal imaging-guided cancer photothermal therapy. *Nanoscale.* 2016;8(39):17150–8.
194. Hardy J, Selkoe DJ. The amyloid hypothesis of Alzheimer's disease: progress and problems on the road to therapeutics. *Science.* 2002;297(5580):353–6.
195. Gao N, et al. Gold-nanoparticle-based multifunctional amyloid- β inhibitor against Alzheimer's disease. *Chemistry.* 2015;21(2):829–35.
196. Gao N, et al. Transition-metal-substituted polyoxometalate derivatives as functional anti-amyloid agents for Alzheimer's disease. *Nat Commun.* 2014;5:3422.
197. Zhang W, et al. Metal-dependent inhibition of amyloid fibril formation: synergistic effects of cobalt-tannic acid networks. *Nanoscale.* 2019;11(4):1921–8.
198. Li W, et al. Mussel byssus-like reversible metal-chelated supramolecular complex used for dynamic cellular surface engineering and imaging. *Adv Func Mater.* 2015;25(24):3775–84.
199. Zhou X, Sun H, Bai X. Two-dimensional transition metal dichalcogenides: synthesis, biomedical applications and biosafety evaluation. *Front Bioeng Biotechnol.* 2020. <https://doi.org/10.3389/fbioe.2020.00236>.
200. Ko MP, Huang CJ. A versatile approach to antimicrobial coatings via metal-phenolic networks. *Colloids Surf B Biointerfaces.* 2020;187:110771.
201. Asgari M, et al. Mg-Phenolic network strategy for enhancing corrosion resistance and osteocompatibility of degradable magnesium alloys. *ACS Omega.* 2019;4(26):21931–44.
202. Liu P, et al. Core-shell nanosystems for self-activated drug-gene combinations against triple-negative breast cancer. *ACS Appl Mater Interfaces.* 2020;12(48):53654–64.
203. Bi J, et al. Immunotoxicity of metal and metal oxide nanoparticles: from toxic mechanisms to metabolism and outcomes. *Biomater Sci.* 2023;11(12):4151–83.
204. Björnmalm M, et al. In vivo biocompatibility and immunogenicity of metal-phenolic gelation. *Chem Sci.* 2019;10(43):10179–94.
205. Markovsky E, et al. Administration, distribution, metabolism and elimination of polymer therapeutics. *J Control Release.* 2012;161(2):446–60.
206. Bourquin J, et al. Biodistribution, clearance, and long-term fate of clinically relevant nanomaterials. *Adv Mater.* 2018;30(19):e1704307.
207. Patton JS, Byron PR. Inhaling medicines: delivering drugs to the body through the lungs. *Nat Rev Drug Discov.* 2007;6(1):67–74.
208. Yun Y, Cho YW, Park K. Nanoparticles for oral delivery: targeted nanoparticles with peptidic ligands for oral protein delivery. *Adv Drug Deliv Rev.* 2013;65(6):822–32.
209. Byun H, et al. Biomimetic anti-inflammatory and osteogenic nanoparticles self-assembled with mineral ions and tannic acid for tissue engineering. *Nano Converg.* 2022;9(1):47.
210. Song X, et al. Biomimetic epigallocatechin gallate-cerium assemblies for the treatment of rheumatoid arthritis. *ACS Appl Mater Interfaces.* 2023;15(28):33239–49.
211. Yang B, et al. Super-assembled core-shell mesoporous silica-metal-phenolic network nanoparticles for combinatorial photothermal therapy and chemotherapy. *Nano Res.* 2020;13(4):1013–9.
212. Torchilin V. Tumor delivery of macromolecular drugs based on the EPR effect. *Adv Drug Deliv Rev.* 2011;63(3):131–5.
213. Ren Z, et al. A Metal-polyphenol-coordinated nanomedicine for synergistic cascade cancer chemotherapy and chemodynamic therapy. *Adv Mater.* 2020;32(6):e1906024.
214. Conner SD, Schmid SL. Regulated portals of entry into the cell. *Nature.* 2003;422(6927):37–44.
215. Doherty GJ, McMahon HT. Mechanisms of endocytosis. *Annu Rev Biochem.* 2009;78:857–902.
216. Zhang W, et al. Cobalt-directed assembly of antibodies onto metal-phenolic networks for enhanced particle targeting. *Nano Lett.* 2020;20(4):2660–6.
217. Mehvar R. Dextran for targeted and sustained delivery of therapeutic and imaging agents. *J Control Release.* 2000;69(1):1–25.
218. Wang Y, et al. A disassembling strategy overcomes the EPR effect and renal clearance dilemma of the multifunctional theranostic nanoparticles for cancer therapy. *Biomaterials.* 2019;197:284–93.
219. Deen WM, Lazzara MJ, Myers BD. Structural determinants of glomerular permeability. *Am J Physiol Renal Physiol.* 2001;281(4):F579–96.
220. Ohlson M, Sörensson J, Haraldsson B. A gel-membrane model of glomerular charge and size selectivity in series. *Am J Physiol Renal Physiol.* 2001;280(3):F396–405.
221. Longmire M, Choyke PL, Kobayashi H. Clearance properties of nanosized particles and molecules as imaging agents: considerations and caveats. *Nanomedicine.* 2008;3(5):703–17.
222. Liu F, et al. Gram-scale synthesis of coordination polymer nanodots with renal clearance properties for cancer theranostic applications. *Nat Commun.* 2015;6:8003.
223. Yang Y, et al. Ligand-directed stearic acid grafted chitosan micelles to increase therapeutic efficacy in hepatic cancer. *Mol Pharm.* 2015;12(2):644–52.
224. Wang L, et al. Characterization of gold nanorods in vivo by integrated analytical techniques: their uptake, retention, and chemical forms. *Anal Bioanal Chem.* 2010;396(3):1105–14.
225. Poelstra K, Prakash J, Beljaars L. Drug targeting to the diseased liver. *J Control Release.* 2012;161(2):188–97.

226. Bartsch M, et al. Massive and selective delivery of lipid-coated cationic lipoplexes of oligonucleotides targeted in vivo to hepatic endothelial cells. *Pharm Res*. 2002;19(5):676–80.
227. Cheong SJ, et al. Superparamagnetic iron oxide nanoparticles-loaded chitosan-linoleic acid nanoparticles as an effective hepatocyte-targeted gene delivery system. *Int J Pharm*. 2009;372(1–2):169–76.
228. Zhang YN, et al. Nanoparticle-liver interactions: cellular uptake and hepatobiliary elimination. *J Control Release*. 2016;240:332–48.
229. Yona S, Gordon S. From the reticuloendothelial to mononuclear phagocyte system - the unaccounted years. *Front Immunol*. 2015;6:328.
230. Liu J, et al. Passive tumor targeting of renal-clearable luminescent gold nanoparticles: long tumor retention and fast normal tissue clearance. *J Am Chem Soc*. 2013;135(13):4978–81.
231. Song XR, et al. Polyphenol-inspired facile construction of smart assemblies for ATP- and pH-responsive tumor MR/optical imaging and photothermal therapy. *Small*. 2017. <https://doi.org/10.1002/smll.201603997>.
232. Zhu W, et al. Metal-organic framework nanoparticle-assisted cryopreservation of red blood cells. *J Am Chem Soc*. 2019;141(19):7789–96.
233. Rahim MA, et al. Phenolic building blocks for the assembly of functional materials. *Angew Chem Int Ed Engl*. 2019;58(7):1904–27.
234. Shen W, et al. Natural polyphenol inspired polycatechols for efficient siRNA delivery. *CCS Chemistry*. 2020;2(3):146–57.
235. Forooshani PK, et al. Hydroxyl radical generation through the fenton-like reaction of hematin- and catechol-functionalized microgels. *Chem Mater*. 2020;32(19):8182–94.
236. Shin M, Park E, Lee H. Plant-inspired pyrogallol-containing functional materials. *Adv Func Mater*. 2019;29(43):1903022.
237. Khare E, Holten-Andersen N, Buehler M. Transition-metal coordinate bonds for bioinspired macromolecules with tunable mechanical properties. *Nat Rev Mater*. 2021;6:421–36.
238. Osterberg R. Origins of metal ions in biology. *Nature*. 1974;249(455):382–3.
239. Holm RH, Kennepohl P, Solomon EI. Structural and functional aspects of metal sites in biology. *Chem Rev*. 1996;96(7):2239–314.
240. Zhou J, et al. Polyphenol-mediated assembly for particle engineering. *Acc Chem Res*. 2020;53(7):1269–78.
241. Wang G, et al. Nanoporous carbon spheres derived from metal-phenolic coordination polymers for supercapacitor and biosensor. *J Colloid Interface Sci*. 2019;544:241–8.
242. Godoy-Gallardo M, et al. Evaluation of bone loss in antibacterial coated dental implants: An experimental study in dogs. *Mater Sci Eng C Mater Biol Appl*. 2016;69:538–45.
243. Geng H, et al. Interfacial assembly of metal-phenolic networks for hair dyeing. *ACS Appl Mater Interfaces*. 2020;12(26):29826–34.
244. Lin G, et al. Selective metal-phenolic assembly from complex multi-component mixtures. *ACS Appl Mater Interfaces*. 2019;11(19):17714–21.
245. Ameloot R, et al. Interfacial synthesis of hollow metal-organic framework capsules demonstrating selective permeability. *Nat Chem*. 2011;3(5):382–7.
246. Wang X, et al. Metal-organic coordination-enabled layer-by-layer self-assembly to prepare hybrid microcapsules for efficient enzyme immobilization. *ACS Appl Mater Interfaces*. 2012;4(7):3476–83.
247. Wang H, et al. Controlled fabrication of functional capsules based on the synergistic interaction between polyphenols and MOFs under weak basic condition. *ACS Appl Mater Interfaces*. 2017;9(16):14258–64.
248. Zhou C, et al. Metal-phenolic self-assembly shielded probiotics in hydrogel reinforced wound healing with antibiotic treatment. *Mater Horiz*. 2023;10(8):3114–23.
249. Yan J, et al. Engineering radiosensitizer-based metal-phenolic networks potentiate STING pathway activation for advanced radiotherapy. *Adv Mater*. 2022;34(10):e2105783.
250. Yan J, et al. Metal-phenolic nanomedicines regulate T-cell anti-tumor function for sono-metabolic cancer therapy. *ACS Nano*. 2023;17(15):14667–77.
251. Zhou X, et al. Metal-phenolic network-encapsulated nanovaccine with pH and reduction dual responsiveness for enhanced cancer immunotherapy. *Mol Pharm*. 2020;17(12):4603–15.
252. Wang Q, et al. Tumor immunomodulatory effects of polyphenols. *Front Immunol*. 2022;13:1041138.
253. Zheng HT, et al. Pegylated metal-phenolic networks for antimicrobial and antifouling properties. *Langmuir*. 2019;35(26):8829–39.
254. Yun G, et al. Synthesis of metal nanoparticles in metal-phenolic networks: catalytic and antimicrobial applications of coated textiles. *Adv Healthc Mater*. 2018. <https://doi.org/10.1002/adhm.201700934>.
255. Anh HTP, Huang CM, Huang CJ. Intelligent metal-phenolic metallogels as dressings for infected wounds. *Sci Rep*. 2019;9(1):11562.
256. Li X, et al. Assembly of metal-phenolic/catecholamine networks for synergistically anti-inflammatory, antimicrobial, and anticoagulant coatings. *ACS Appl Mater Interfaces*. 2018;10(47):40844–53.
257. Chen Y, et al. Injectable nanofiber microspheres modified with metal phenolic networks for effective osteoarthritis treatment. *Acta Biomater*. 2023;157:593–608.
258. Fan G, et al. Metal-phenolic networks as versatile coating materials for biomedical applications. *ACS Appl Bio Mater*. 2022. <https://doi.org/10.1021/acsabm.2c00136>.
259. Qin J, et al. Recent advances of metal-polyphenol coordination polymers for biomedical applications. *Biosensors*. 2023. <https://doi.org/10.3390/bios13080776>.
260. Xu W, et al. Direct assembly of metal-phenolic network nanoparticles for biomedical applications. *Angew Chem Int Ed Engl*. 2023;62(45):e202312925.
261. Lin Z, et al. Metal-phenolic network composites: from fundamentals to applications. *Chem Soc Rev*. 2024;53(22):10800–26.
262. Wang X, et al. Engineering polyphenol-based polymeric nanoparticles for drug delivery and bioimaging. *Chem Eng J*. 2022;439:135661.
263. Han Y, et al. Polyphenol-mediated assembly of proteins for engineering functional materials. *Angew Chem Int Ed Engl*. 2020;59(36):15618–25.
264. Zhao Z, et al. Engineering of living cells with polyphenol-functionalized biologically active nanocomplexes. *Adv Mater*. 2020;32(49):e2003492.
265. Xie Y, et al. Alloyed nanostructures integrated metal-phenolic nanoplat-form for synergistic wound disinfection and revascularization. *Bioact Mater*. 2022;16:95–106.
266. Li H-Y, et al. Inorganic-polymer composite coatings for biomedical devices. *Smart Mater Med*. 2021;2:1–14.

Publisher's Note

Springer Nature remains neutral with regard to jurisdictional claims in published maps and institutional affiliations.